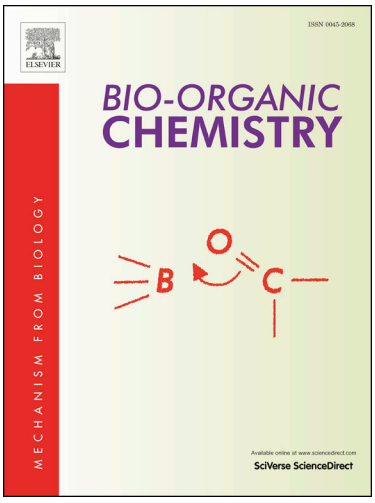

Synthesis, *in vitro* and *in vivo* biological evaluation of dihydroartemisinin derivatives with potential anti-*Toxoplasma gondii* agents

Hao Deng, Xing Huang, Chunmei Jin, Chun-Mei Jin, Zhe-Shan Quan

PII: S0045-2068(19)31006-5
DOI: https://doi.org/10.1016/j.bioorg.2019.103467
Reference: YBIOO 103467

To appear in: *Bioorganic Chemistry*

Received Date: 24 June 2019
Revised Date: 9 October 2019
Accepted Date: 21 November 2019

Please cite this article as: H. Deng, X. Huang, C. Jin, C-M. Jin, Z-S. Quan, Synthesis, *in vitro* and *in vivo* biological evaluation of dihydroartemisinin derivatives with potential anti-*Toxoplasma gondii* agents, *Bioorganic Chemistry* (2019), doi: https://doi.org/10.1016/j.bioorg.2019.103467

Synthesis, *in vitro* and *in vivo* biological evaluation of dihydroartemisinin derivatives with potential anti-*Toxoplasma gondii* agents

Hao Deng[a], Xing Huang[a], Chunmei Jin[a], Chun-Mei Jin[a]* & Zhe-Shan Quan[a]*

[a]Key Laboratory of Natural Resources and Functional Molecules of the Changbai Mountain, Affiliated Ministry of Education, College of pharmacy, Yanbian University, Yanji, Jilin, China;

***Corresponding author: Tel: + 86 433 243-6020; Fax: + 86 433 243-6020.**

E-mail: zsquan@ybu.edu.cn (Z. S. Quan).

***Corresponding author:**

E-mail: cmjin@ybu.edu.cn (C. M. Jin).

Abstract

In this study, four series of dihydroartemisinin derivatives were designed, synthesized, and evaluated for anti-toxoplasma gondii activity, and calculated the selectivity index (SI). It was the higher the SI, the better the effect of this compound against *Toxoplasma gondii*. Our goal was to filter out compounds that were bigger SI than the lead compound. The compound with the highest SI was selected for the anti-toxoplasmosis test in mice *in vivo*. Among the synthesized compounds, the (*3R,5aS,6R,8aS,9R,12R,12aR*)-3,6,9-trimethyl-decahydro-12*H*-3,12-epoxy[1,2]di-oxepino[4,3-*i*]isochromen-10-yl-(*te*-*rt*-butoxycarbonyl)-*L*-alaninate (A2) exhibited the most potent anti-*T. gondii* activity and low cytotoxicity (SI: 6.44), yielding better results than the lead compound DHA (SI: 1.00) and the clinically used positive-control drug spiramycin (SI: 0.72) *in vitro*. Furthermore, compound A2 had better growth inhibitory effects on *T. gondii in vivo* than spiramycin did and significantly reduced the number of tachyzoites in the peritoneal cavity of mice ($P<0.01$). The evaluation of the data generated in the *T. gondii* mouse infection model indicates that compound A2 treatment was a good inhibitor of *T. gondii in vivo* and that it was effective in relieving the liver damage induced by *T. gondii*. In addition, the results of a docking study revealed that A2 could become a better *T. gondii* calcium-dependent protein kinase1 (*Tg*CDPK1) inhibitor. For this reason, compound A2 has potential as an anti-parasitic drug. Further studies are required to elucidate the mechanism of the action of compound A2, as well as to develop drug delivery systems for patients.

Keywords: Dihydroartemisinin derivatives, *Toxoplasma gondii*, *In vitro*, *In vivo*.

1. Introduction

Toxoplasma gondii (*T. gondii*), a protozoan parasite, has a global distribution and can infect virtually all homeothermic animals [1]. It is estimated to infect 2 billion people worldwide [2] with South America having the highest infection rates [3], which is likely to be correlated with people's lifestyles and eating habits. When ingested by mammals, it can increase the rate of abortion and stillbirth [4]. Although hosts with normal immune function present with no obvious symptoms upon *Toxoplasma* infection, parasites can cause the most serious and even life-threatening damage in people with immune deficiencies [5].

T. gondii has a complex life cycle, multifarious pathogenesis, and different biological characteristics so that no medicine has been developed to date that is fully effective and can completely eradicate toxoplasmosis. Clinical drugs used against toxoplasmosis are pyrimethamine, sulfadiazine, and spiramycin. The combination of sulfadiazine and pyrimethamine has obvious anti-parasitic effects [6], but it causes a number of severe side effects, such as thrombocytopenia, liver and kidney complications [7], bone marrow toxicity [8]. Due to the current shortcomings of toxoplasmosis treatment drugs, there is an urgent need to develop a drug that is highly effective, has low toxicity and few side effects.

Natural products are sources rich in active compounds against *T. gondii* activity. Dihydroartemisinin (DHA) is obtained by hydrogenation-reduction of artemisinin (Fig. 1. a.) that is extracted from the traditional Chinese medicine *Artemisia annua* L. and has a variety of pharmacological activities, including anti-malarial [9], anti-tumor [10, 11], and anti-viral [12] activities. In addition to these important pharmacological activities, it was found that DHA also has anti-*T. gondii* activity [13, 14]. However, studies have shown that DHA has low solubility in water

and short half-life [15].

Hybridization of two or more pharmacophore units with different mechanisms of action within the same molecule is rationally attractive [16]. Many natural products increase activity significantly after the introduction of amino acids [17, 18]. As the basic structure of the protein, introduction of amino acid fragments into lead compounds may enhance their ability to bind to anti-*T. gondii* targets. In the present study, compound I increased its activity against *T. gondii* due to the introduction of amino acids into arctigenin[19].

Cinnamic acid and 2-indole carboxylic acid have many activities, including anticancer [20, 21], antibacterial [22], antiparasitic [23, 24]. The skeleton of compound II is cinnamic acid, and the compound exhibits good anti-*T. gondii* activity [25]. The LD_{50} of Compound III containing an indole ring was 57 μM against *T. gondii*, demonstrating the Toxoplasma killing activity of this compound [26].

Moreover, nitrogen-containing heterocycle such as quinoline or secondary amino-heterocycles has also been reported to have anti-*T. gondii* activity [27]. Compound IV has an ED_{50} of 78.6 nM against *T. gondii* and exhibits extremely strong antiparasitic activity [29]. In summary, as shown in Fig. 2, we designed several dihydroartemisinin derivatives containing active fragment as described above, which are expected to obtain better activity against *T. gondii* derivatives.

Therefore, in this study, we used the principle of molecule combination to design and synthesize novel DHA derivatives and evaluated theirs *in vitro* anti-*T. gondii* activity using a previously established method [28]. We obtained a compound named A2 (Fig. 1. b.) with good activity anti-*T. gondii* and low toxicity and evaluated related indicators to further validate its anti-*T. gondii* activity *in vivo*.

Materials and Methods

2.1 Experimental compounds

2.1.1 General procedures

All chemicals and spectral grade solvents were obtained commercially and were used without further purification. Solvent were dried and used according to standard procedures. All chemical reactions were monitored by thin-layer chromatography (TLC). The melting points of all compounds were determined by capillary method (temperature uncorrected). The ^{1}H NMR and ^{13}C NMR spectra were determined on a BRUKER AV-300 (Bruker, Switzerland) using Deuterated dimethyl sulfoxide (DMSO) as the solvent and the chemical shift unit is ppm. High resolution mass spectra of the compounds were determined by Thermo Scientific LTQ Orbitrap XL.

2.1.2 Procedure for the preparation of compound A1-A6, B1-B6, C1-C4

A solution of DHA (0.5 mmol) and appropriate carboxyl compounds (1.0 mmol) in dry DCM (5 mL) was treated with 1-(3-dimethylaminopropyl)-3-ethylcarbodiimide hydrochloride (EDCI) (1.0 mmol) and N,N-dimethylaminopyridine (DMAP) (0.5 mmol). The mixture was stirred 5-8 h at room temperature. Until the reaction completed, it was extracted with DCM and the organic phase was washed with 10% sodium bicarbonate solution and saturated brine, and dried over Na_2SO_4. The solid was removed by filtration and the solvent was evaporated under reduced pressure to afford the crude product that was further purificated by column chromatography (DCM : methanol = 200:1 - 75:1, V/V) to give a white solid. And further characterized by the physical and spectroscopic data shown below.

(3R,5aS,6R,8aS,9R,12R,12aR)-3,6,9-trimethyldecahydro-12H-3,12-epoxy[1,2]dioxepino[4,3-i]isochromen-10-yl (tert-butoxycarbonyl)glycinate ***(A1)***

M.p. 108-109 ℃. Yield: 51%; ^{1}H NMR (300 MHz, DMSO-d_6): δ 7.31 (t, J = 5.9 Hz, 1H,N-H), 5.69 (d, J = 9.7 Hz, 1H, 12-H), 5.58 (s, 1H,10-H), 3.76 (d, J = 6.0 Hz, 2H, -CH_2-), 2.37-2.12 (m, 3H), 2.00 (d, J = 14.2 Hz, 1H), 1.80(s, 1H), 1.68-1.51 (m, 5H), 1.39 (s, 9H, $(CH_3)_3$), 1.29 (s, 4H), 1.20 (dd, J = 11.1, 6.2 Hz, 1H), 0.89(d, J = 6.1 Hz, 3H), 0.78 (d, J = 7.1 Hz, 3H); ^{13}C NMR (75 MHz, DMSO-d_6): δ 169.77, 156.30, 104.06, 92.58, 91.09, 80.31, 78.81, 51.57, 44.99, 42.40, 36.39, 36.35, 34.16, 33.80, 32.11, 28.61 (3C), 25.97, 21.45, 20.51, 12.09; ESI-HRMS (*m/z*) calcd for $C_{22}H_{36}NO_8^+$ $[M+H]^+$ 442.2435, found: 442.2436.

(3R,5aS,6R,8aS,9R,12R,12aR)-3,6,9-trimethyldecahydro-12H-3,12-epoxy[1,2]dioxepino[4,3-i]isochromen-10-yl (tert-butoxycarbonyl)-L-alaninate ***(A2)***

M.p. 113-114 ℃. Yield: 49%; ^{1}H NMR (300 MHz, DMSO-d_6): δ 7.39 (d, J = 7.5 Hz, 1H, N-H), 6.23 (d, J = 4.0 Hz, 1H, 12-H), 5.43 (s, 1H, 10-H), 4.10-4.00 (m, 1H, -CH-), 2.22 (dd, J = 31.2, 13.9 Hz, 3H), 2.07-1.93 (m, 2H), 1.80 (s, 2H), 1.70 -1.51 (m, 4H), 1.38 (s, 9H, -CH_3), 1.28 (s, 4H), 1.25 (s, 3H, -CH_3), 0.89 (d, J = 6.2 Hz, 3H), 0.78 (d, J = 7.1 Hz, 3H); ^{13}C NMR (75 MHz, DMSO-d_6): δ 172.34, 155.63, 104.00, 92.63, 91.08, 80.31, 78.69, 51.60, 49.44, 45.06, 36.43, 36.33, 34.19, 32.25, 28.65 (3C), 25.96, 24.66, 21.47, 20.51, 16.98, 12.11; ESI-HRMS (*m/z*) calcd for $C_{23}H_{38}NO_8^+$ $[M+H]^+$ 456.2591, found: 456.2590.

(3R,5aS,6R,8aS,9R,12R,12aR)-3,6,9-trimethyldecahydro-12H-3,12-epoxy[1,2]dioxepino[4,3-

i]isochromen-10-yl (tert-butoxycarbonyl)-L-valinate ***(A3)***

M.p. 117-118 ℃. Yield: 48%; ^{1}H NMR (300 MHz, DMSO-d_6): δ 7.29 (d, J = 8.3 Hz, 1H, N-H), 5.69 (d, J = 9.6 Hz, 1H, 12-H), 5.56 (s, 1H, 10-H), 3.91-3.80 (m, 1H, -CH-), 2.32 (s, 1H), 2.25-2.11 (m, 1H), 2.03 (dd, J = 17.0, 10.3 Hz, 2H), 1.81 (d, J = 7.2 Hz, 1H), 1.56 (m, 5H), 1.38 (d, J = 8.1 Hz, 9H, -CH_3), 1.26 (s, 3H), 1.24-1.11 (m, 2H), 0.98-0.87 (m, 9H, ,-CH_3), 0.79 (d, J = 7.0 Hz, 3H); ^{13}C NMR (75 MHz, DMSO-d_6): δ 171.33, 156.17, 103.93, 92.62, 90.95, 80.26, 78.72, 59.99, 51.57, 45.09, 36.44, 36.28, 34.20, 32.09, 29.92, 28.67 (3C), 25.93, 24.68, 21.46, 20.51, 19.42, 18.82, 12.17; ESI-HRMS (*m/z*) calcd for $C_{25}H_{42}NO_8^+$ $[M+H]^+$ 484.2910, found: 484.2909.

(3R,5aS,6R,8aS,9R,12R,12aR)-3,6,9-trimethyldecahydro-12H-3,12-epoxy[1,2]dioxepino[4,3-i]isochromen-10-yl (tert-butoxycarbonyl)-L-leucinate ***(A4)***

M.p. 122-123 ℃. Yield: 59%; ^{1}H NMR (300 MHz, DMSO-d_6): δ 7.35 (d, J = 7.9 Hz, 1H, N-H), 5.67 (d, J = 9.7 Hz, 1H, 12-H), 5.57 (s, 1H,10-H), 4.01 (s, 1H, -CH-), 2.30 (s, 1H), 2.16 (m, 1H), 2.00 (m, 2H), 1.84-1.78 (m, 1H), 1.68-1.51 (m, 7H), 1.37 (d, J = 7.3 Hz, 9H, -CH_3), 1.28 (s, 4H), 1.19 (dd, J = 10.6, 6.4 Hz, 2H), 0.93-0.84 (m, 9H), 0.78 (d, J = 6.9 Hz, 3H); ^{13}C NMR (75 MHz, DMSO-d_6): δ 172.22, 155.93, 136.13, 103.98, 92.64, 91.06, 80.30, 78.71, 52.46, 51.59, 45.06, 36.43, 36.32, 34.19, 32.24, 28.65 (3C), 25.94, 24.66, 24.63, 23.23, 21.67, 21.48, 20.51, 12.11; ESI-HRMS (*m/z*) calcd for $C_{26}H_{44}NO_8^+$ $[M+H]^+$ 498.3066, found: 498.3067.

(3R,5aS,6R,8aS,9R,12R,12aR)-3,6,9-trimethyldecahydro-12H-3,12-epoxy[1,2]dioxepino[4,3-i]isochromen-10-yl (tert-butoxycarbonyl)-L-methioninate ***(A5)***

M.p. 166-168 ℃. Yield: 56%; ^{1}H NMR (300 MHz, DMSO-d_6): δ 7.42 (d, J = 7.9 Hz, 1H, N-H),

5.68 (d, J = 9.7 Hz, 1H, 12-H), 5.57 (s, 1H, 10-H), 4.13 (m, 1H, -CH_2-), 2.31 (s, 1H), 2.25-2.12 (m, 2H), 2.05 (s, 2H), 1.94-1.82 (m, 3H, S-CH_3), 1.80 (s, 1H), 1.67-1.47 (m, 7H), 1.39 (s, 9H, CH_3), 1.28 (s, 4H), 1.20 (m, 2H), 0.89 (d, J = 6.2 Hz, 3H), 0.79 (d, J = 7.1 Hz, 3H); ^{13}C NMR (75 MHz, DMSO-d_6): δ 171.67, 155.94, 103.99, 92.78, 91.03, 80.28, 78.85, 52.97, 51.57, 45.04, 36.44, 36.31, 34.19 , 32.15, 30.60, 29.93, 28.64 (3C), 25.93, 24.67, 21.46, 20.50, 15.00, 12.12; ESI-HRMS (*m/z*) calcd for $C_{25}H_{42}NO_8S^+$ $(M+H)^+$ 516.2625, found: 516.2626.

(3R,5aS,6R,8aS,9R,12R,12aR)-3,6,9-trimethyldecahydro-12H-3,12-epoxy[1,2]dioxepino[4,3-i]isochromen-10-yl (tert-butoxycarbonyl)-L-phenylalaninate ***(A6)***

M.p. 114-115 ℃. Yield: 72%; ^{1}H NMR (300 MHz, DMSO-d_6): δ 7.35 (s, 1H, N-H), 7.27 (s, 5H, Ar-H), 5.70 (d, J = 9.3 Hz, 1H, 12-H), 5.59 (s, 1H, 10-H), 4.20 (s, 1H, -CH-), 3.11-2.85(m, 2H, -CH_2-), 2.33 (s, 1H), 2.17 (d, J = 12.7 Hz, 1H), 2.01 (d, J = 11.8 Hz, 1H), 1.81 (s, 1H), 1.72-1.49 (m, 5H), 1.33 (s, 9H, -CH_3), 1.29 (s, 4H), 1.25-1.15 (m, 2H), 0.85 (d, J = 28.3 Hz, 6H); ^{13}C NMR (75 MHz, DMSO-d_6): δ 171.21, 155.73, 138.06, 129.68 (2C), 128.62 (2C), 126.85, 104.01, 92.86, 91.10, 80.32, 78.78, 55.53, 51.60, 45.07, 36.42, 36.34, 36.24, 34.29, 32.21 , 28.59 (3C), 25.95, 24.68, 21.47, 20.52, 12.13; ESI-HRMS (*m/z*) calcd for $C_{29}H_{42}NO_8^+$ $[M+H]^+$ 532.2910, found: 532.2911.

(3R,5aS,6R,8aS,9R,12R,12aR)-3,6,9-trimethyldecahydro-12H-3,12-epoxy[1,2]dioxepino[4,3-i]isochromen-10-yl cinnamate ***(B1)***

M.p. 120-122℃; Yield: 89%; ^{1}H NMR (300 MHz, DMSO-d_6) δ 7.80 (d, J = 16.0 Hz, 1H), 7.56 (q, 2H, Ar-H), 7.49-7.35 (m, 3H, Ar-H), 6.52 (d, J = 16.0 Hz, 1H), 5.95 (d, J = 9.8 Hz, 1H, 12-H), 5.52 (s, 1H, 10-H), 2.70 (dd, J = 9.0, 5.5 Hz, 1H), 2.42 (td, J = 14.0, 3.9 Hz, 1H), 2.07 (dd, J = 9.0, 5.6

Hz, 1H), 1.97 - 1.89 (m, 1H), 1.87 - 1.63 (m, 3H), 1.58 (s, 1H), 1.53 (d, *J* = 7.6 Hz, 1H), 1.46 (s, 3H, 13-CH_3), 1.39 -1.26 (m, 2H), 1.00 (d, *J* = 5.7 Hz, 3H), 0.92 (d, *J* = 7.1 Hz, 3H). ^{13}C NMR (75 MHz, DMSO-d_6) δ 165.36, 146.37, 134.33, 131.24, 129.41(2C), 129.05(2C), 117.92, 104.06, 92.34, 91.08, 80.37, 51.60, 45.10, 36.44,36.37, 34.19, 32.12, 25.98, 24.68, 21.52, 20.54, 12.34; ESI-HRMS (*m/z*) calcd for $C_{22}H_{36}NO_8^+$ $[M+H]^+$ 442.2435, found: 442.2436.

(3R,5aS,6R,8aS,9R,12R,12aR)-3,6,9-trimethyldecahydro-12H-3,12-epoxy[1,2]dioxepino[4,3-i]isochromen-10-yl (E)-3-(4-fluorophenyl)acrylate ***(B2)***

M.p. 110-111℃; Yield: 86%; ^{1}H NMR (300 MHz, DMSO-d_6) δ 7.87 (q, 2H, Ar-H), 7.77 (d, *J* = 16.1 Hz, 1H), 7.28 (t, 2H, Ar-H), 6.71 (d, *J* = 16.1 Hz, 1H), 5.80 (d, *J* = 9.7 Hz, 1H, 12-H), 5.62 (s, 1H, 10-H), 2.47 - 2.36 (m, 1H), 2.21 (dd, *J* = 18.9, 8.5 Hz, 1H), 2.01 (d, *J* = 14.1 Hz, 1H), 1.82 (d, *J* = 7.4 Hz, 1H), 1.62 (dd, *J* = 24.6, 7.6 Hz, 3H), 1.52 - 1.39 (m, 2H), 1.29 (s, 3H, 13-CH_3), 1.26 - 1.12 (m, 2H), 0.90 (d, *J* = 6.2 Hz, 3H), 0.83 (d, *J* = 7.1 Hz, 3H); ^{13}C NMR (75 MHz, DMSO-d_6) δ 165.32, 163.95 (d, *J* = 248.25), 145.13, 131.46 (d, *J* = 8.7 Hz)(2C), 131.05 (d, *J* = 3.1 Hz), 117.82 (d, *J* = 2.2 Hz), 116.44(d, *J* = 21.75)(2C), 104.06, 92.34, 91.08, 80.36, 51.61, 45.10, 36.45, 36.45 , 34.20, 32.12, 25.97, 24.68, 21.53, 20.53, 12.32; ESI-HRMS (*m/z*) calcd for $C_{24}H_{30}FO_6^+$ $[M+H]^+$ 433.2026, found: 433.2027.

(3R,5aS,6R,8aS,9R,12R,12aR)-3,6,9-trimethyldecahydro-12H-3,12-epoxy[1,2]dioxepino[4,3-i]isochromen-10-yl (E)-3-(4-chlorophenyl)acrylate ***(B3)***

M.p. 100-102℃; Yield: 79%; ^{1}H NMR (300 MHz, DMSO-d_6) δ 7.82 (d, *J* = 8.5 Hz, 2H, Ar-H), 7.76 (d, *J* = 16.1 Hz, 1H), 7.51 (d, *J* = 8.5 Hz, 2H, Ar-H), 6.77 (d, *J* = 16.1 Hz, 1H), 5.80 (d, *J* = 9.8

Hz, 1H, 12-H), 5.62 (s, 1H, 10-H), 2.40 (d, *J* = 7.3 Hz, 1H), 2.18 (dd, *J* = 19.0, 8.6 Hz, 1H), 2.01 (d, *J* = 14.2 Hz, 1H), 1.81 (s, 1H), 1.69 -1.55 (m, 3H), 1.52 - 1.35 (m, 2H), 1.29 (s, 3H, 13-CH_3), 1.21 (dd, *J* = 11.0, 5.8 Hz, 2H), 0.90 (d, *J* = 6.2 Hz, 3H), 0.83 (d, *J* = 7.1 Hz, 3H); ^{13}C NMR (75 MHz, DMSO-d_6) δ 165.24, 144.95, 135.76, 133.33, 130.79(2C), 129.46(2C),118.77 104.06, 92.41, 91.08, 80.36, 51.61, 45.09, 36.43, 36.36, 34.20, 32.12,25.97, 24.68, 21.51, 20.54, 12.32; ESI-HRMS (*m/z*) calcd for $C_{24}H_{30}ClO_6^+$ $[M+H]^+$ 449.1730, found: 449.1731.

(3R,5aS,6R,8aS,9R,12R,12aR)-3,6,9-trimethyldecahydro-12H-3,12-epoxy[1,2]dioxepino[4,3-i]isochromen-10-yl (E)-3-(4-bromophenyl)acrylate ***(B4)***

M.p. 95-96℃; Yield: 80%; ^{1}H NMR (300 MHz, DMSO-d_6) δ 7.77 (d, *J* = 16.1 Hz, 1H), 7.73 (d, *J* = 5.1 Hz, 2H, Ar-H), 7.64 (d, *J* = 8.5 Hz, 2H, Ar-H), 6.78 (d, *J* = 16.1 Hz, 1H), 5.80 (d, *J* = 9.8 Hz, 1H, 12-H), 5.62 (s, 1H, 10-H), 2.41 (s, 1H), 2.26 - 2.13 (m, 1H), 2.01 (d, *J* = 13.7 Hz, 1H), 1.81 (s, 1H), 1.69 - 1.56 (m, 3H), 1.54 - 1.39 (m, 2H), 1.29 (s, 3H, 13-CH_3), 1.25 - 1.12 (m, 2H), 0.90 (d, *J* = 6.3 Hz, 3H), 0.83 (d, *J* = 7.1 Hz, 3H); ^{13}C NMR (75 MHz, DMSO-d_6) δ 165.24, 145.05, 133.66, 132.39 (2C), 130.98 (2C), 124.65, 118.84, 104.07, 92.42, 91.09, 80.36, 51.61, 45.10, 36.46,36.37, 34.19, 32.11, 25.97, 24.68, 21.52, 20.53, 12.32; ESI-HRMS (*m/z*) calcd for $C_{24}H_{30}BrO_6^+$ $[M+H]^+$ 493.1225, found: 493.1227.

(3R,5aS,6R,8aS,9R,12R,12aR)-3,6,9-trimethyldecahydro-12H-3,12-epoxy[1,2]dioxepino[4,3-i]isochromen-10-yl (E)-3-(4-methoxyphenyl)acrylate ***(B5)***

M.p. 90-91℃; Yield: 84%; ^{1}H NMR (300 MHz, DMSO-d_6) δ 7.75 (s, 2H，Ar-H), 7.70 (s, *J* = 16.0 Hz, 1H), 7.01 (s, 2H，Ar-H), 6.58 (d, *J* = 16.0 Hz, 1H), 5.80 (d, *J* = 8.6 Hz, 1H), 5.61 (s, 1H), 3.81

(s, 3H), 2.51 (s, 1H), 2.41 (s, 1H), 2.21 (s, 1H), 2.03 (s, 1H), 1.82 (s, 1H), 1.62 (d, J = 11.3 Hz, 3H), 1.47 (s, 2H), 1.29 (s, 3H, 13-CH_3), 1.25 (s, 2H), 0.87 (d, J = 20.7 Hz, 6H); ^{13}C NMR (75 MHz, DMSO-d_6) δ 165.62, 161.87, 146.18, 130.91 (2C), 126.98, 115.12, 114.89 (2C), 104.04, 92.14, 91.05, 80.37, 55.83, 51.62, 45.11, 36.45, 36.38, 34.21, 32.13, 25.98, 24.68, 21.55, 20.54, 12.35. ESI-HRMS (*m/z*) calcd for $C_{25}H_{33}O_7^+$ $[M+H]^+$ 445.2226, found: 445.2225.

(3R,5aS,6R,8aS,9R,12R,12aR)-3,6,9-trimethyldecahydro-12H-3,12-epoxy[1,2]dioxepino[4,3-i]isochromen-10-yl (E)-3-(3,4-dimethoxyphenyl)acrylate ***(B6)***

M.p. 85-86 ℃; Yield: 83%; ^{1}H NMR (300 MHz, DMSO-d_6) δ 7.69 (d, J = 15.9 Hz, 1H), 7.42 (s, 1H, Ar-H), 7.31 (d, J = 8.3 Hz, 1H, Ar-H), 7.00 (d, J = 8.3 Hz, 1H, Ar-H), 6.65 (d, J = 15.9 Hz, 1H), 5.80 (d, J = 9.7 Hz, 1H, 10-H), 5.61 (s, 1H, 10-H), 3.79 (t, J = 7.0 Hz, 6H, -OCH_3), 2.41 (s, 1H), 2.26 - 2.14 (m, 1H), 2.01 (d, J = 12.5 Hz, 1H), 1.81 (s, 1H), 1.67 - 1.55 (m, 3H), 1.49 (s, 2H), 1.29 (s, 3H, 13-CH_3), 1.26 - 1.14 (m, 2H), 0.90 (d, J = 6.2 Hz, 3H), 0.83 (d, J = 7.1 Hz, 3H); ^{13}C NMR (75 MHz, DMSO-d_6) δ 165.67, 151.72, 149.47, 146.56, 127.20, 123.79, 115.33, 111.97, 110.99, 104.04, 92.11, 91.03, 80.36, 56.08, 56.07, 51.61, 45.12, 36.47, 36.38, 34.20, 32.13, 25.98, 24.69, 21.54, 20.54, 12.36; ESI-HRMS (*m/z*) calcd for $C_{26}H_{35}O_8^+$ $[M+H]^+$ 475.2331, found: 475.2333.

(3R,5aS,6R,8aS,9R,12R,12aR)-3,6,9-trimethyldecahydro-12H-3,12-epoxy[1,2]dioxepino[4,3-i]isochromen-10-yl 1H-indole-2-carboxylate ***(C1)***

M.p. 98-99 ℃. Yield: 57%; ^{1}H NMR (300 MHz, DMSO-d_6): δ 12.02 (s, 1H, N-H), 7.69 (d, J = 8.0 Hz, 1H, Ar-H), 7.49 (d, J = 8.3 Hz, 1H, Ar-H), 7.36-7.26 (m, 2H, Ar-H), 7.10 (t, J = 7.5 Hz, 1H,

Ar-H), 5.91 (d, *J* = 9.7 Hz, 1H, 12-H), 5.67 (s, 1H, 10-H), 2.55 (m, 1H), 2.27-2.15 (m, 1H), 2.01 (d, *J* = 15.2 Hz, 1H), 1.90-1.78 (m, 1H), 1.73-1.59 (m, 3H), 1.43 (m, 3H), 1.29 (s, 3H), 1.22 (m, 2H), 0.90 (t, *J* = 6.8 Hz, 6H); ^{13}C NMR (75 MHz, DMSO-d_6): δ 160.31, 138.23, 127.16, 126.78, 125.55, 122.6, 120.83, 113.18, 109.53, 92.65, 91.20, 80.41, 51.64, 45.12, 36.43, 36.37, 34.20, 32.21, 25.96, 24.68, 21.57, 20.54, 12.33; ESI-HRMS (*m/z*) calcd for $C_{24}H_{29}NO_6Na^+$ $[M+Na]^+$ 450.1887, found: 450.1891.

(3R,5aS,6R,8aS,9R,12R,12aR)-3,6,9-trimethyldecahydro-12H-3,12-epoxy[1,2]dioxepino[4,3-i]isochromen-10-yl 5-chloro-1H-indole-2-carboxylate ***(C2)***

M.p. 126-127 ℃. Yield: 45%; ^{1}H NMR (300 MHz, DMSO-d_6): δ 12.23 (s, 1H, N-H), 7.76 (d, *J* = 1.7 Hz, 1H, Ar-H), 7.50 (d, *J* = 8.8 Hz, 1H, Ar-H), 7.30 (dd, *J* = 9.0, 1.9 Hz, 2H, Ar-H), 5.91 (d, *J* = 9.7 Hz, 1H, 12-H), 5.67 (s, 1H, 10-H), 2.53(s, 1H), 2.19 (dd, *J* = 19.0, 8.7 Hz, 1H), 2.01 (d, *J* = 14.2 Hz, 1H), 1.83 (d, *J* = 7.8 Hz, 1H), 1.63 (m, 3H), 1.45 (m, 3H), 1.28 (s, 3H), 1.21 (m, 2H), 0.88 (d, *J* = 7.4 Hz, 6H); ^{13}C NMR (75 MHz, DMSO-d_6): δ 160.03, 136.56, 128.22, 128.10, 125.73, 125.34, 121.70, 114.88, 109.02, 104.11, 92.86, 91.22, 80.41, 51.63, 45.10, 36.44, 36.37, 34.20, 32.20, 25.96, 24.69, 21.56, 20.55, 12.32; ESI-HRMS (*m/z*) calcd for $C_{24}H_{29}ClNO_6^+$ $(M+H)^+$ 462.1677, found: 462.1677.

(3R,5aS,6R,8aS,9R,12R,12aR)-3,6,9-trimethyldecahydro-12H-3,12-epoxy[1,2]dioxepino[4,3-i]isochromen-10-yl 6-bromo-1H-indole-2-carboxylate ***(C3)***

M.p. 116-118 ℃. Yield: 47%; ^{1}H NMR (300 MHz, DMSO-d_6): δ 12.17 (s, 1H, N-H), 7.67 (d, *J* = 9.0 Hz, 2H, Ar-H), 7.33 (s, 1H, Ar-H), 7.25 (d, *J* = 8.5 Hz, 1H, Ar-H), 5.91 (d, *J* = 9.4 Hz, 1H, 12-

H), 5.68 (s, 1H, 10-H), 2.53(s, 1H), 2.19 (d, *J* = 13.0 Hz, 1H), 2.02 (d, *J* = 13.8 Hz, 1H), 1.83 (s, 1H), 1.64 (d, *J* = 12.3 Hz, 3H), 1.40 (d, *J* = 40.6 Hz, 3H), 1.29 (s, 3H), 1.19 (d, *J* = 7.4 Hz, 2H), 0.88 (dd, *J* = 15.8, 8.2 Hz, 6H); ^{13}C NMR (75 MHz, DMSO-d_6): δ 160.06, 138.83, 127.64, 126.12, 124.63, 123.99, 118.45, 115.57, 109.70, 104.10, 92.84, 91.22, 80.39, 51.61, 45.09, 36.43, 36.36, 34.19, 32.21, 25.96, 24.67, 21.55, 20.53, 12.31; ESI-HRMS (*m/z*) calcd for $C_{24}H_{29}BrNO_6^+$ $[M+H]^+$ 506.1178, found: 506.1179.

(3R,5aS,6R,8aS,9R,12R,12aR)-3,6,9-trimethyldecahydro-12H-3,12-epoxy[1,2]dioxepino[4,3-i]isochromen-10-yl 5-methoxy-1H-indole-2-carboxylate ***(C4)***

M.p. 165-166 ℃. Yield: 65%; ^{1}H NMR (300 MHz, DMSO-d_6): δ 11.89 (s, 1H, N-H), 7.38 (d, *J* = 9.0 Hz, 1H, Ar-H), 7.16 (d, *J* = 20.4 Hz, 2H, Ar-H), 7.01-6.90 (m, 1H, Ar-H), 5.89 (d, *J* = 9.8 Hz, 1H, 12-H), 5.67 (s, 1H, 10-H), 3.77 (s, 3H, -OCH_3), 2.53(s, 1H), 2.29-2.15 (m, 1H), 2.01 (d, *J* = 15.5 Hz, 1H), 1.82 (s, 1H), 1.64 (d, *J* = 13.8 Hz, 3H), 1.58-1.35 (m, 3H), 1.29 (s, 3H), 1.27-1.09 (m, 2H), 0.89 (dd, *J* = 9.3, 6.8 Hz, 6H); ^{13}C NMR (75 MHz, DMSO-d_6): δ 160.21, 154.53, 133.61, 127.48, 126.90, 117.34, 114.10, 109.05, 104.10, 102.41, 92.56, 91.19, 80.43, 55.69, 51.65, 45.12, 36.43, 36.38, 34.22, 32.22, 25.97, 24.69, 21.57, 20.56, 12.34; ESI-HRMS (*m/z*) calcd for $C_{25}H_{32}NO_7^+$ $[M+H]^+$ 458.2173, found: 458.2178.

2.1.3 Procedure for the preparation of compound D

A solution of dihydroartemisinin (2.0 g, 7.04 mmol) in anhydrous dichloromethane (75 mL) was stirred at 0℃. Succinic anhydride (845 mg, 8.45 mmol) and anhydrous piperidine (2.1 mL, 21.12 mmol) were added and the solution was stirred from 0℃ to 25℃ for 2 hours. The reaction

mixture was washed with 10% HCl, The crude mixture was purified by flash column chromatography using 1-2% methanol / dichloromethane / 1% acetic acid as eluent to get white solid ***(D)***, (yield: 85%), and further characterized by the physical and spectroscopic data shown below.

M.p. 140-142 ℃ Yield: 85%; ^{1}H NMR (300 MHz, DMSO-d_6): δ 12.26 (s, 1H, -OH), 5.67 (d, J = 9.7 Hz, 1H, 12-H), 5.57 (s, 1H, 10-H), 2.67-2.53 (m, 4H, -CH_2-), 2.29 (s, 1H), 2.17 (d, J = 10.0 Hz, 1H), 2.00 (d, J = 13.7 Hz, 1H), 1.80 (s, 1H), 1.61 (d, J = 9.8 Hz, 3H), 1.56-1.38 (m, 3H), 1.29 (s, 3H, 13-CH_3), 1.26-1.12 (m, 2H), 0.89 (d, J = 6.3 Hz, 3H, -CH_3), 0.77 (d, J = 7.1 Hz, 3H, -CH_3).

2.1.4 Procedure for the preparation of compound E1-E10

A 25 mL round bottomed flask was charged with D (100 mg, 0.26 mmol), heterocyclic rings (0.51 mmol), EDCI (0.51 mmol) and DMAP (0.26 mmol) and DCM (5 mL). This reaction mixture was stirred at room temperature for 5~8 h. The mixture was extracted with DCM and the organic phase was washed with saturated sodium bicarbonate solution and brine, and dried over Na_2SO_4. The solid was removed by filtration and the solvent was evaporated under reduced pressure to afford the crude product further purified by chromatography (DCM : MeOH= 100:1~30:1) and characterized by the physical and spectroscopic data shown below.

(3R,5aS,6R,8aS,9R,12R,12aR)-3,6,9-trimethyldecahydro-12H-3,12-epoxy[1,2]dioxepino[4,3-i]isochromen-10-yl 4-oxo-4-(quinolin-5-ylamino)butanoate ***(E1)***

M.p. 124-125 ℃. Yield: 49%; ^{1}H NMR (300 MHz, DMSO-d_6): δ 10.53 (s, 1H, N-H), 8.89 (d, J =

2.4 Hz, 1H, Ar-H), 8.70 (s, 1H, Ar-H), 7.93 (t, *J* = 8.5 Hz, 2H, Ar-H), 7.60 (dt, *J* = 14.8, 6.8 Hz, 2H, Ar-H), 5.69 (d, *J* = 9.7 Hz, 1H, 12-H), 5.56 (s, 1H, 10-H), 2.76 (s, 4H, -CH_2-),2.31 (s, 1H), 2.18 (t, *J* = 12.0 Hz, 1H), 2.05-1.95 (m, 1H), 1.79 (s, 1H), 1.59 (d, *J* = 8.8 Hz, 3H), 1.53-1.36 (m, 3H), 1.29 (s, 3H, 13-CH_3), 1.25-1.13 (m, 2H), 0.87 (d, *J* = 6.2 Hz, 3H), 0.77 (d, *J* = 7.0 Hz, 3H); ^{13}C NMR (75 MHz, DMSO-d_6): δ 171.61, 171.10, 144.78, 144.57, 133.32, 128.99, 128.34, 128.15, 128.11, 127.50, 122.20, 104.05, 92.24, 91.08, 80.33, 51.58, 45.04, 36.43, 36.36, 34.15, 32.11, 31.08, 29.10, 25.99, 24.64, 21.47, 20.49, 12.18; ESI-HRMS (*m/z*) calcd for $C_{28}H_{35}N_2O_7^+$ $[M+H]^+$ 511.2438, found: 511.2444.

(3R,5aS,6R,8aS,9R,12R,12aR)-3,6,9-trimethyldecahydro-12H-3,12-epoxy[1,2]dioxepino[4,3-i]isochromen-10-yl 4-oxo-4-(quinolin-5-ylamino)butanoate ***(E2)***

M.p. 149-150 ℃. Yield: 40%; ^{1}H NMR (300 MHz, DMSO-d_6): δ 10.14 (s, 1H, N-H), 8.91 (d, *J* = 2.7 Hz, 1H, Ar-H), 8.50 (d, *J* = 8.4 Hz, 1H, Ar-H), 7.85 (d, *J* = 6.7 Hz, 1H, Ar-H), 7.80-7.69 (m, 2H, Ar-H), 7.56 (q, 1H), 5.71 (d, *J* = 9.8 Hz, 1H, 12-H), 5.58 (s, 1H, 10-H), 2.88-2.72 (m, 4H, -CH_2-),2.31 (s, 1H), 2.26-2.12 (m, 1H), 2.01 (d, *J* = 11.1 Hz, 1H), 1.87-1.75 (m, 1H), 1.69-1.54 (m, 3H), 1.46 (d, *J* = 8.7 Hz, 3H), 1.29 (s, 3H, 13-CH_3), 1.24-1.09 (m, 2H), 0.89 (d, *J* = 6.2 Hz, 3H), 0.77 (d, *J* = 7.1 Hz, 3H); ^{13}C NMR (75 MHz, DMSO-d_6): δ 171.74, 171.05, 150.88, 148.59, 134.40, 132.03, 129.52 (2C), 126.49, 121.86, 121.31, 104.05, 92.22, 91.08, 80.34, 51.60, 45.05, 36.44, 36.38, 34.18, 32.15 , 30.75 , 29.37, 26.00, 24.66, 21.47, 20.52, 12.23; ESI-HRMS (*m/z*) calcd for $C_{28}H_{35}N_2O_7^+$ $[M+H]^+$ 511.2438, found: 511.2444.

(3R,5aS,6R,8aS,9R,12R,12aR)-3,6,9-trimethyldecahydro-12H-3,12-epoxy[1,2]dioxepino[4,3-

i]isochromen-10-yl 4-oxo-4-(quinolin-8-ylamino)butanoate ***(E3)***

M.p. 156-157 ℃. Yield: 43%; ^{1}H NMR (300 MHz, DMSO-d_6): δ 10.21 (s, 1H, N-H), 8.94 (dd, J = 4.2, 1.6 Hz, 1H, Ar-H), 8.60 (d, J = 7.6 Hz, 1H, Ar-H), 8.41 (dd, J = 8.3, 1.6 Hz, 1H, Ar-H), 7.69-7.61 (m, 2H, Ar-H), 7.57 (t, J = 7.9 Hz, 1H, Ar-H), 5.69 (d, J = 9.8 Hz, 1H, 12-H), 5.55 (s, 1H, 10-H), 2.93 (t, J = 6.3 Hz, 2H, -CH_2-), 2.82-2.71 (m, 2H, -CH_2-), 2.29 (d, J = 6.5 Hz, 1H), 2.17 (d, J = 13.7 Hz, 1H), 1.99 (d, J = 13.0 Hz, 1H), 1.85-1.76 (m, 1H), 1.59 (d, J = 10.2 Hz, 3H), 1.44 (dd, J = 25.3, 16.4 Hz, 3H), 1.29 (s, 3H, 13-CH_3), 1.25-1.11 (m, 2H), 0.87 (d, J = 6.2 Hz, 3H), 0.77 (d, J = 7.1 Hz, 3H); ^{13}C NMR (75 MHz, DMSO-d_6): δ 171.69, 170.76, 149.26, 138.55, 137.01, 135.04, 128.31, 127.41, 122.54, 122.23, 117.16, 104.03, 92.20, 91.06, 80.32, 51.58, 45.05, 36.42, 36.36, 34.16, 32.12, 31.57, 29.29, 25.99, 24.65, 21.47, 20.50, 12.18; ESI-HRMS (*m/z*) calcd for $C_{28}H_{35}N_2O_7^+$ $[M+H]^+$ 511.2438, found: 511.2444.

quinolin-3-yl ((3R,5aS,6R,8aS,9R,12R,12aR)-3,6,9-trimethyldecahydro-12H-3,12-epoxy[1,2]dio-xepino[4,3-i]isochromen-10-yl) succinate ***(E4)***

M.p. 126-127 ℃.Yield: 34%; ^{1}H NMR (300 MHz, DMSO-d_6): δ 8.74 (d, J = 2.6 Hz, 1H, Ar-H), 8.18 (d, J = 2.4 Hz, 1H, Ar-H), 8.13-7.97 (m, 2H, Ar-H), 7.86-7.74 (m, 1H, Ar-H), 7.66 (t, J = 7.5 Hz, 1H, Ar-H), 5.73 (d, J = 9.8 Hz, 1H, 12-H), 5.59 (s, 1H, 10-H), 3.01 (t, J = 6.2 Hz, 2H, -CH_2-),2.85 (m, 2H, -CH_2-), 2.33 (s, 1H), 2.26-2.12 (m, 1H), 2.01 (dd, J = 16.2, 5.6 Hz, 1H), 1.88-1.76 (m, 1H), 1.70-1.55 (m, 3H), 1.54-1.37 (m, 3H), 1.27 (s, 3H, -CH_3), 1.26-1.10 (m, 2H), 0.89 (d, J = 6.2 Hz, 3H), 0.78 (d, J = 7.1 Hz, 3H); ^{13}C NMR (75 MHz, DMSO-d_6): δ 171.49, 171.27, 146.44, 144.35, 129.79, 129.22, 128.42, 128.30, 127.89, 126.75, 104.07, 98.53, 92.50, 91.11, 80.34, 51.59, 45.03, 36.42, 36.36, 34.17, 32.13,31.57, 29.16, 25.97, 24.66, 21.46, 20.52, 12.22; ESI-HRMS (*m/z*)

calcd for $C_{28}H_{34}NO_8^+$ [M+H]$^+$ 512.2278, found: 512.2279.

quinolin-5-yl ((3R,5aS,6R,8aS,9R,12R,12aR)-3,6,9-trimethyldecahydro-12H-3,12-epoxy[1,2]dioxepino[4,3-i]isochromen-10-yl) succinate ***(E5)***

M.p. 87-88 ℃.Yield: 30%; ^{1}H NMR (300 MHz, DMSO-d_6): δ 8.97 (d, J = 2.6 Hz, 1H, Ar-H), 8.37 (d, J = 8.5 Hz, 1H, Ar-H), 7.97 (d, J = 8.4 Hz, 1H, Ar-H), 7.79 (t, J = 8.0 Hz, 1H, Ar-H), 7.60 (q, 1H, Ar-H), 7.41 (d, J = 7.5 Hz, 1H, Ar-H), 5.74 (d, J = 9.6 Hz, 1H, 12-H), 5.60 (s, 1H, 10-H), 3.10 (t,J = 6.4 Hz, 2H, -CH_2-), 2.90 (t, J = 6.4 Hz, 2H, -CH_2-), 2.33 (s, 1H), 2.26-2.13 (m, 1H), 2.01 (d, J = 13.6 Hz, 1H), 1.81 (s, 1H), 1.69-1.56 (m, 3H), 1.46 (m, 3H), 1.28 (s, 3H, 13-CH_3), 1.22 (d, J = 11.6 Hz, 2H), 0.89 (d, J = 5.9 Hz, 4H), 0.78 (d, J = 6.9 Hz, 3H); ^{13}C NMR (75 MHz, DMSO-d_6): δ 171.48, 171.32, 151.60, 146.39, 130.51, 129.95, 129.57, 127.50, 122.35, 119.38, 104.07, 92.53, 91.13, 80.34, 51.59, 45.02, 36.43, 34.37, 34.17, 32.13, 29.20, 29.10, 25.98, 24.66, 21.46, 20.52, 12.22; ESI-HRMS (*m/z*) calcd for $C_{28}H_{34}NO_8^+$ [M+H]$^+$ 512.2278, found: 512.2279.

.

quinolin-8-yl ((3R,5aS,6R,8aS,9R,12R,12aR)-3,6,9-trimethyldecahydro-12H-3,12-epoxy[1,2]dioxepino[4,3-i]isochromen-10-yl) succinate ***(E6)***

M.p. 74-76 ℃.Yield: 39%; ^{1}H NMR (300 MHz, DMSO-d_6): δ 8.91 (dd, J = 4.2, 1.5 Hz, 1H, Ar-H), 8.50-8.41 (dd, J = 8.3, 1.5 Hz 1H, Ar-H), 7.92 (d, J = 8.2 Hz, 1H, Ar-H), 7.67-7.58 (m, 2H, Ar-H), 7.53 (d, J = 7.6 Hz, 1H, Ar-H), 5.72 (d, J = 9.7 Hz, 1H, 12-H), 5.60 (s, 1H), 3.06 (t, J = 6.4 Hz, 2H, -CH_2-), 2.85 (t, J = 6.4 Hz, 2H, -CH_2-), 2.32 (s, 1H), 2.17 (d, J = 10.3 Hz, 1H), 2.01 (d, J = 14.6 Hz, 1H), 1.81 (s, 1H), 1.67-1.55 (m, 3H), 1.47 (d, J = 12.0 Hz, 3H), 1.29 (s, 3H, 13-CH_3), 1.20 (dd, J = 11.2, 6.4 Hz, 2H), 0.89 (d, J = 6.2 Hz, 3H), 0.76 (d, J = 7.1 Hz, 3H); ^{13}C NMR (75 MHz, DMSO-

d_6): δ 171.22, 171.11, 151.10, 147.31, 140.89, 136.71, 129.56, 126.87, 126.61, 122.60, 121.99, 104.06, 92.43, 91.11, 80.34, 51.59, 45.05, 36.43, 36.36, 34.17, 32.11, 29.31, 28.99, 25.99, 24.66, 21.47, 20.52, 12.21; ESI-HRMS (*m/z*) calcd for $C_{28}H_{34}NO_8^+$ $[M+H]^+$ 512.2278, found: 512.2279.

(3R,5aS,6R,8aS,9R,12R,12aR)-3,6,9-trimethyldecahydro-12H-3,12-epoxy[1,2]dioxepino[4,3-i]isochromen-10-yl 4-(diethylamino)-4-oxobutanoate ***(E7)***

M.p. 130-131 ℃ Yield: 43%; ^{1}H NMR (300 MHz, DMSO-d_6): δ 5.65 (d, J = 9.7 Hz, 1H, 12-H), 5.55 (s, 1H, 10-H), 3.32-3.21 (m, 4H, -CH_2-), 2.59 (s, 4H, -CH_2-), 2.36-2.25 (m, 1H), 2.24-2.13 (m, 1H), 2.00 (d, J = 14.1 Hz, 1H), 1.87-1.76 (m, 1H), 1.68-1.53 (m, 3H), 1.45 (m, 3H), 1.29 (s, 3H, 13-CH_3), 1.26-1.16 (m, 2H), 1.13 (t, J = 7.0 Hz, 3H, -CH_3), 1.00 (t, J = 7.0 Hz, 3H, -CH_3), 0.89 (d, J = 6.2 Hz, 3H, -CH_3), 0.76 (d, J = 7.1 Hz, 3H, -CH_3); ^{13}C NMR (75 MHz, DMSO-d_6): δ 171.78, 169.92, 104.02, 91.99, 91.03, 80.33, 51.60, 45.06, 41.52, 39.87, 36.44, 36.37, 32.14, 29.54, 27.51, 25.98, 24.67, 21.48, 20.53, 14.43, 13.52, 12.16; ESI-HRMS (*m/z*) calcd for $C_{23}H_{38}NO_7^+$ $[M+H]^+$ 440.2648, found: 440.2649.

(3R,5aS,6R,8aS,9R,12R,12aR)-3,6,9-trimethyldecahydro-12H-3,12-epoxy[1,2]dioxepino[4,3-i]isochromen-10-yl 4-morpholino-4-oxobutanoate ***(E8)***

oil, Yield: 50 %; ^{1}H NMR (300 MHz, DMSO-d_6): δ 5.65 (d, J = 9.8 Hz, 1H, 12-H), 5.55 (s, 1H, 10-H), 3.61-3.51 (m, 4H, -CH_2-), 3.45 (m, 4H, -CH_2-), 2.61 (s, 4H, -CH_2-), 2.30 (s, 1H), 2.25-2.13 (m, 1H), 2.00 (d, J = 14.6 Hz, 1H), 1.80 (s, 1H), 1.61 (d, J = 11.8 Hz, 3H), 1.53-1.38 (m, 3H), 1.29 (s, 3H, -CH_3), 1.26-1.10 (m, 2H), 0.89 (d, J = 6.1 Hz, 3H, -CH_3), 0.77 (d, J = 7.1 Hz, 3H, -CH_3); ^{13}C NMR (75 MHz, DMSO-d_6): δ 171.74, 169.91, 104.03, 92.05, 91.05, 80.34, 66.53 (2C), 51.60, 45.59,

45.06, 42.06, 36.44, 36.36, 34.18, 32.16, 29.37, 27.47, 25.99, 24.66, 21.48, 20.53, 12.18; ESI-HRMS (*m/z*) calcd for $C_{23}H_{36}NO_8^+$ $[M+H]^+$ 454.2440, found: 454.2441.

(3R,5aS,6R,8aS,9R,12R,12aR)-3,6,9-trimethyldecahydro-12H-3,12-epoxy[1,2]dioxepino[4,3-i]isochromen-10-yl 4-oxo-4-(4-phenylpiperazin-1-yl)butanoate ***(E9)***

M.p. 144-145 ℃.Yield: 55%; ^{1}H NMR (300 MHz, DMSO-d_6): δ 7.23 (t, J = 7.7 Hz, 2H, Ar-H), 6.95 (d, J = 8.1 Hz, 2H, Ar-H), 6.81 (t, J = 7.2 Hz, 1H, Ar-H), 5.65 (d, J = 9.7 Hz, 1H, 12-H), 5.55 (s, 1H, 10-H), 3.59 (s, 4H), 3.15 (s, 2H, -CH_2-), 3.08(s, 2H, -CH_2-), 2.64 (d, J = 11.2 Hz, 4H, -CH_2-), 2.28 (s, 1H), 2.16 (d, J = 14.4 Hz, 1H), 1.99 (d, J = 15.4 Hz, 1H), 1.79 (s, 1H), 1.60 (m, 3H), 1.47 (m, 3H), 1.29 (s, 3H, -CH_3), 1.21 (d, J = 20.8 Hz, 2H), 0.88 (d, J = 5.9 Hz, 3H, -CH_3), 0.77 (d, J = 6.7 Hz, 3H, -CH_3); ^{13}C NMR (75 MHz, DMSO-d_6): δ 171.77, 169.71, 151.28, 129.46 (2C), 119.78, 116.32 (2C), 104.04, 92.05, 91.05, 80.35, 51.61, 49.13, 48.76, 45.05, 44.95, 41.51, 36.43, 36.37, 34.18, 32.15, 29.43, 27.61, 25.99, 24.66, 21.47, 20.53, 12.21; ESI-HRMS (*m/z*) calcd for $C_{29}H_{41}N_2O_7^+$ $[M+H]^+$ 529.2908, found: 529.2909.

(3R,5aS,6R,8aS,9R,12R,12aR)-3,6,9-trimethyldecahydro-12H-3,12-epoxy[1,2]dioxepino[4,3-i]isochromen-10-yl 4-(4-benzylpiperazin-1-yl)-4-oxobutanoate ***(E10)***

M.p. 136-138 ℃.Yield: 53%; ^{1}H NMR (300 MHz, DMSO-d_6): δ 7.32 (s, 5H), 5.64 (d, J = 9.7 Hz, 1H, 12-H), 5.55 (s, 1H, 10-H), 3.49 (s, 2H, -CH_2-), 3.45 (s, 4H, -CH_2-), 2.59 (s, 4H, -CH_2-), 2.34 (m, 4H, -CH_2-), 2.25 (m, 1H), 2.17 (d, J = 11.5 Hz, 1H), 2.00 (d, J = 13.2 Hz, 1H), 1.80 (s, 1H), 1.60 (d, J = 11.2 Hz, 3H), 1.53-1.36 (m, 3H), 1.29 (s, 3H, -CH_3), 1.25-1.13 (m, 2H), 0.89 (d, J = 5.8 Hz, 3H, -CH_3), 0.76 (d, J = 6.8 Hz, 3H, -CH_3); ^{13}C NMR (75 MHz, DMSO-d_6): δ 171.73, 169.51,

138.31, 132.78, 129.34 (2C), 128.67 (2C), 127.47, 104.03, 92.03, 91.05, 80.34, 62.35, 53.16, 52.74, 51.62, 45.07, 41.69, 36.44, 36.39, 34.20, 32.15, 29.43, 27.60, 26.00, 24.67, 21.49, 20.53, 12.20; ESI-HRMS (*m/z*) calcd for $C_{23}H_{35}NO_8Na^+$ $[M+Na]^+$ 476.2254, found: 476.2256.

2.2 Cell line maintenance

HeLa cells were cultured in DMEM, supplemented with 100 units/mL Penicillin and 100 μg/mL streptomycin and 10% heat-inactivated FBS and maintained at 37℃ and 5% CO_2. Cells were from Molecular Drug Research Center, Yanbian University.

2.3. Parasite strains

This experiment used the virulent RH strain of *T. gondii* that were cryopreserved and resuscitated by our laboratory and maintained by serial intraperitoneal passage in KM female mice, which were purchased from Experiment Center, Yanbian University.

2.4 Animals

All experimental procedures were conducted in conformity with institutional guidelines for the care and use of laboratory animals in Yanbian University, Jilin, China, and conformed to the National Institutes of Health Guide for Care and Use of Laboratory Animals (Number of license SCXK 2011-0007). All mice were kept in a central animal care facility with free access to water and rodent food during the experiment.

2.5 Evaluation of anti-Toxoplasma activity in vitro

Cells were plated in 96-well plates at appropriate densities to ensure exponential growth throughout the experimental period (3×10^3 cells per well) and then allowed to adhere for 24 h at 37°C. The cells were infected with *T. gondii* (1.5×10^4 tachyzoites/well), and then *T. gondii*-infected cells were incubated for 24 h. All compounds were stocked at the concentration of 100 mM in DMSO. Serial dilutions (1~1000 μmol/L) of each compound were tested. The final concentration of DMSO solvent did not exceed 0.01%. After 24 h of incubation, 10 μL of MTT (Thiazolyl Blue Tetrazolium Bromide, 3-(4,5-dimethyl-2-thiazolyl)-2,5-diphenyl-2-H -tetrazolium bromide) solution (5 mg/ml) was added to each well. Plates were then incubated for a further 3.5-4 h. IC_{50} in HeLa cells, IC_{50} in *T. gondii* and selectivity index (Selectivity) were calculated by Excel software. Selectivity index was a measure of specific resistance to *T. gondii*. Calculated using the formula shown in Table 2.

2.6 In vivo experiments

Thirty female mice were randomly divided into five groups: normal group, untreated group (infected untreated group), infected with 100 mg/kg spiramycin-treated group, infected with A2-treated group and infected with DHA-treated groups, six in each group and then intraperitoneally injected with 2×10^3 tachyzoites of the *T. gondii* RH strain. Four hours after the mice were infected, they were gavaged at a dose of 100 mg/kg, while the normal and untreated group was given the same dose of physiological saline. Administered once a day for 4 consecutive days. At the last day, heart blood samples were collected after anesthesia to separate the serum, and then mice were sacrificed by cervical dislocation. The number of tachyzoites in the abdominal cavity of the mice was counted under the light microscope and the inhibition rate of the parasites was calculated.

2.7 Liver biochemical parameters

Serum levels of aspartate transaminase (AST) and alanine aminotransferase (ALT) were measured according to the method of [29]. The substrate reaction of ALT or AST and serum was carried out under incubation at 37 ℃ for 30 min, then added 2,4-dinitrophenylhydrazine (2,4-DNPH) and held for 20 min. Finally, NaOH was added and allowed to react for 5 min. The absorbance at 505 nm was measured.

The glutathione (GSH) was measured according to the method of [30]. The liver homogenate was mixed with half volume trichloroacetic acid (20%, w/v) and centrifuged at 4000 rpm for 10 min. Then, phosphate buffer (phosphate 0.3 mol/L, pH 7.5) and 5,5-dithio-bis-(2-nitrobenzoic acid) (0.04%, w/v) were added to the separated supernatant and mixed thoroughly. After 5 min at room temperature, the absorbance was measured at 412 nm. Malondialdehyde (MDA) was measured by the standard method [31] with minor modifications. The liver homogenate supernatant was mixed with thiobarbituric acid (0.5%, w/v) and heated in boiling water bath for 1 h, then cooled quickly and centrifuged at 6000 rpm for 10 min, the absorbance of pink colored supernatant was measured at 532 nm. Tetraethoxypropane replaced the liver homogenate in the standard sample.

2.8 The molecular docking study

The molecular docking study was performed using Discovery Studio (DS) 2017. The ligand and protein were prepared, hydrogen was added and water molecules were deleted by DS Server. The result of docking was treated with DS Client. In this study, the crystal structure of *T. gondii* calcium-dependent Protein Kinase 1 from Toxoplasma gondii (*Tg*CDPK1, 3N51. pdb) was chosen for docking. The xyz coordinates (19.4414, 14.3063, 63.6324, radius 9.9 Å) of protein residues were defined as the binding site sphere. The protocol, Dock Ligant (CDOKER) was used to perform the

docking. The output poses of the ligands generated were analysed based on the LibDockScore function.

3. Results and discussion

3.1 Chemistry

Natural products play a leading role in drug discovery and structural modifications of active natural products is an effective way of discovering potentially active molecules, lead compounds, and new drugs. Modification of the natural compounds is used to be potential anti-*T. gondii* agents [32-35]. DHA, a sesquiterpene natural compound containing peroxy bridge bond (R-O-O-R'), which was found to have anti-*T. gondii* activity [13, 14]. The outlines for the synthesis of the starting and of the target compounds are presented in Scheme 1 and Table 1. Due to the light sensitive nature of the peroxy bridge structure in DHA and its derivatives [36], all compounds should be stored in the dark in dry conditions.

In order to react with the 12-OH of DHA, we first need to protect the amino group of the amino acid with di-*tert*-butyl dicarbonate (Boc_2O). *N*-Boc amino acids were synthesized by the reaction of amino acid and Boc_2O under NaOH catalytic conditions [37]. Synthetic cinnamic acid and 2-indole carboxylic acid are all based on substituted benzaldehyde. Synthetic cinnamic acid requires one step reaction, while 2-indole carboxylic acid requires three steps, so the yield of cinnamic acid was much higher than that of 2-indole carboxylic acid [38, 39].

The reagents EDCI and DMAP play a fundamental role in the condensation reactions of carboxyl and amino or hydroxyl groups. In addition to their role in accelerating the chemical reaction, these reagents circumvent the unfavorable formation of water and promote the reaction to proceed in the forward direction. We can increase one of the raw materials to increase the yields. The yield of A1-A7, B1-B6, and C1-C4 was 40%-89%, and the yield of E1-E10 was 29%-55%.

3.2 Evaluation of biological activities

3.2.1 Evaluation of anti-Toxoplasma activity in vitro (MTT assay)

MTT assay was used to determine the cytotoxicity and the anti-*T. gondii* activity of DHA and derivatives on host cells (Table 2). *In vitro*, the anti-*T. gondii* activity was expressed as the selectivity index (SI), which was calculated as the ratio between the CC_{50} value for host cells non-infected with *Toxoplasma* and the IC_{50} for *T. gondii* cultivated in host cells (SI= CC_{50} / IC_{50}) [28, 40]. When the SI level is higher than data of spiramycin, and the toxicity of the compound to the host cells (HeLa cells) is lower and the compound reduces the infection of the host cells by *T. gondii*, the compounds are thought to dwell better anti-*T.gondii* activity effect [28]. As shown in Table 2, compounds A1, A2, A5, B1, B3, B4, C2, E1, E2, E4, E6, E7, E9, and E10 exhibited stronger anti-*T. gondii* activity than the lead compound DHA (SI: 1.00). Furthermore, when compared to the clinical toxoplasmosis drug spiramycin, most of the compounds showed stronger anti-parasitic activity, with selectivity indexes from 0.83 to 6.44.

Compounds A1-A6 were products of the reaction of *N*-Boc amino acids with DHA. Compared with lead compound DHA, toxicity (IC_{50} in HeLa Cells) of most compounds was reduced. Within compounds A1, A2, A3 and A4, compound A2, which was the product of the reaction of alanine with DHA, demonstrated the strongest anti-*T. gondii* capacity, suggesting that it can interfere with the binding of *T. gondii* to its key targets with high selectivity. The compounds B1-B6 were the products of the reaction of cinnamic acids and DHA, and almost all compounds were less toxic to host cells than that of DHA. Among them selectivity index of compounds B1, B3 and B4 was greater than that of spiramycin, indicating that these three compounds were the better safety than spiramycin. The compounds C1-C4 were the products of the reaction of indole-2-carboxylic acids and DHA. As

shown in Table 2, the toxicity of the four target compounds was higher than the unmodified DHA, probably due to the multiple other activities and targets of the indole fragment [41, 42]. However, the selectivity index of all compounds except C4 was greater than that of spiramycin and showed some anti-*T. gondii* activity. Compounds E1~E10 are products of the reaction of succinic acid with substituted heterocycles. The selectivity of the group was greater than 0.72, and they all exhibited higher anti-*T. gondii* activity than spiramycin. Interestingly, comparison of the aminoquinoline with the corresponding hydroxyquinoline revealed that the aminoquinoline forms have lower toxicity. In short, the compound A2 was the best choice in these compounds for further studies *in vivo*.

3.2.2 The number of tachyzoites in vivo

To examine whether compound A2 was also anti-*T. gondii* effects *in vivo*, we evaluated by counting the number of *T. gondii* in each group of mice' abdominal cavities [43]. The number of intraperitoneal tachyzoites in the untreated (infected untreated group) mice was 2.25×10^6. After treatment with 100 mg/kg spiramycin, the number of tachyzoites in the abdominal cavity of the mice was reduced to approximately 1.06×10^6, and the inhibition rate was 53.1%. Thus, this treatment can significantly reduce the number of tachyzoites ($P < 0.05$). The inhibition rate of DHA was 40.6%, indicating that DHA had a weaker ability to inhibit tachyzoites than spiramycin ($P < 0.05$). The number of tachyzoites in ascitic fluid of compound A2 treated mice significantly reduced, with the inhibitory rates being 70.8% ($P < 0.01$) (Table 3) (Fig. 3). The results showed that A2 had better inhibitory effects on *T. gondii in vivo* than DHA and 100 mg/kg spiramycin did. This showed that A2 has a better effect in inhibiting *T. gondii in vivo*.

3.2.3 Liver and spleen index

Liver has been shown to be the major site of tissue pathology during acute, lethal toxoplasmosis in mice [44], while the spleen plays an important role in coordinating both adaptive and innate immune responses [45]. For these reasons, liver and spleen indices were used to evaluate the protective effect of drugs on viscera. As shown in Figure 4, compared with the normal group, the liver index of the mice infected by *T. gondii* increased slightly, while the spleen index increased significantly. The spleen index of mice in the untreated group was significantly higher than that of the normal group, indicating that splenomegaly of the immune-related organ had been caused by acute *T. gondii* infection ($P < 0.05$). Compared with the normal group, there was improvement of the splenomegaly of the low-dose spiramycin-, DHA- and compound A2-treated groups ($P < 0.05$), after administration of the compounds in the infected mice. This showed that compound A2 can effectively relieve the splenomegaly caused by *T. gondii* infection.

3.2.4 ALT and AST

The liver is the body's largest gland organ. In addition to detoxifying various metabolites, synthesizing proteins and biochemicals necessary for digestion, it also has a central role in the pathophysiology of parasitic infection [46]. The level of serum ALT and AST activity is a very sensitive indicator used to evaluate liver injury, whereby their increase reflects to some extent the degree of the damage (Fig. 5). Compared with the normal group, the serum ALT level was increased in the untreated mice, indicating that acute Toxoplasma infection can cause liver damage. Spiramycin, DHA and A2 can relieve liver damage and slightly reduce enzyme levels ($P< 0.05$). Similarly, compared with the untreated group, the AST content of all the treated groups were significantly reduced ($P < 0.05$). Although DHA and A2 could significantly reduce the number of

tachyzoites in the mouse peritoneal cavity, there was significant difference in the ALT and AST levels in the serum of the DHA and A2 groups ($P< 0.05$) compared with that in the normal group, showing they could not completely reduce the serum ALT and AST levels.

3.2.5 MDA and GSH

MDA is the major degradation product of lipid peroxidation and can cause changes in the structure of hepatocytes, leading to their swelling and necrosis [47]. MDA content reflects the degree of damage of liver cells from another angle [48]. When the liver is damaged, it undergoes a large amount of lipid peroxidation. Acute toxoplasmosis in humans can damage many tissues and organs including the liver and can cause a series of liver pathological changes including hepatitis, hepatomegaly and hepatic granuloma [49-51]. GSH, the major non-protein thiol in humans and other mammals, can react with peroxides to exert antioxidative effects and reduce liver damage [52]. Compared with the normal group, the GSH content in the liver homogenate of the untreated group was significantly decreased ($P<0.01$), and the acute *Toxoplasma gondii* infection caused the decrease of the antioxidant GSH in mice (Fig. 3). Compared to that in the untreated group, DHA and Compound A2 could increase the GSH content, where compound A2 had a significant effect ($P< 0.01$), indicating that the drug can increase the amount of GSH and protect the liver. The content of MDA was increased by acute Toxoplasma infection ($P< 0.01$). Compound A2 had obviously stronger effect than spiramycin in reducing the content of the harmful substance MDA ($P< 0.01$), but DHA did not. Therefore, we can know compound A2 can reduce the body damage caused by Toxoplasma gondii by increasing the content of protective factor GSH and reducing the content of damage factor MDA.

3.3 Docking analysis

It has been reported in the literature that dihydroartemisinin acts on calcium channel-dependent proteins of Toxoplasma gondii to be anti-*T. gondii* [53]. CDPKs are a serine/threonine-like protein kinase that is directly regulated by Ca^{2+} and is not dependent on Calmodulin (CaMs) and phospholipids. We used the computer-aided drug design software Discovery Studio 2017 Server for molecular model construction and protein structure treatment to complete the docking of the target compounds with the calcium-dependent Protein Kinase 1 from *Toxoplasma gondii* (*Tg*CDPK1, 3N51. pdb) (Fig. 7, 8). The compound with the strongest anti-*T. gondii* activity was selected for the molecular docking experiments. Thus, compound A2 and receptor protein preprocessing were performed using the corresponding modules in the Discovery Studio 2017 Client running on the server. Meanwhile, the lead compound DHA also was docked with target protein to prove the difference between its activity of anti-*T. gondii* and A2. The docking process was performed according to the CDOCKER protocol, where the technical parameter Pose Cluster Radius was reset to 0.5 and the other parameters were unchanged. Docking of the active site was set to the coordinates x = 19.4414, y = 14.3063, and z = 63.6324 as the center, with a radius of 9.9 Å. It can be found that the docking results of compound A2 and DHA with target protein were as follows (Table 4): 'at this time, the CDOCKER Interaction energy value of compound A2 was -50.9219 kcal/mol'. Clearly, compound A2 may interact with receptor proteins residue LYS80 and MET112 which The bond lengths between A2 were 3.07, 2.87, 3.05 and 2.39. At the same time, the CDOCKER Interaction energy value of DHA was -28.4487 kcal/mol. DHA may interact with receptor proteins residue TRY131 which The bond lengths between DHA was 1.89. These data indicated that the compound A2 has stronger binding affinity to *Tg*CDPK1 than DHA and may play a key role in anti-*T.gondii* activity. In addition, it is suggested that the structure of DHA may have a better binding effect on

the *Tg*CDPK1 receptor protein, thereby exerting its anti-toxoplasmosis activity, and therefore has further structural modification value.

4. Conclusion

In this study, four series of dihydroartemisinin derivatives were synthesized and evaluated for their anti-*T. gondii* activity *in vitro.* Most of the target compounds not only had activity against *T. gondii* but also had lower toxicity towards the host cells. Compound A2 was the best choice for *in vivo* experiments and could effectively kill *Toxoplasma gondii* tachyzoites in the peritoneal cavity of mice. All effects of in *vivo* experiment were similar or superior to those of the positive-control drug spiramycin. In addition, the results of a docking study revealed that compound A2 could become a better *T. gondii* calcium-dependent protein kinase 1 inhibitor. Hence, the DHA-derived compound A2 had the potential for becoming an anti-parasitic drug, pending further in-depth mechanistic studies.

Acknowledgments

This work was supported by the National Natural Science Foundation of China (No. 21662036, 81160409).

Conflicts of interest

The authors declare that no competing interests exist

References

[1] J.P. Dubey, J. Brown, M. Ternent, S.K. Verma, D.E. Hill, C.K. Cerqueira-Cezar, O.C.H. Kwok, R. Calero-Bernal, J.G. Humphreys, Seroepidemiologic study on the prevalence of Toxoplasma gondii and Trichinella spp. infections in black bears (Ursus americanus) in Pennsylvania, USA, Vet Parasitol 229 (2016) 76-80.

[2] M. Di Cristina, Z. Dou, M. Lunghi, G. Kannan, M.H. Huynh, O.L. McGovern, T.L. Schultz, A.J. Schultz, A.J. Miller, B.M. Hayes, W. van der Linden, C. Emiliani, M. Bogyo, S. Besteiro, I. Coppens, V.B. Carruthers, Toxoplasma depends on lysosomal consumption of autophagosomes for persistent infection, Nat Microbiol 2 (2017) 17096.

[3] J.P. Dubey, J.L. Jones, Toxoplasma gondii infection in humans and animals in the United States, Int J Parasitol 38 (2008) 1257-78.

[4] C. Rudin, K. Boubaker, P.A. Raeber, B. Vaudaux, H.C. Bucher, J.G. Garweg, I. Hoesli, C. Kind, P. Hohlfeld, S.W.G. Conge, Toxoplasmosis during pregnancy and infancy A new approach of Switzerland, Swiss Medical Weekly 138 (2008) 1-8.

[5] V.O. Osunkalu, S.A. Akanmu, N.J. Ofomah, I.V. Onyiaorah, A.A. Adediran, R.O. Akinde, I.A. Onwuezobe, Seroprevalence of Toxoplasma gondii IgG antibody in HIV-infected patients at the Lagos University Teaching Hospital, HIV AIDS (Auckl) 3 (2011) 101-105.

[6] E. Schoondermark-van de Ven, T. Vree, W. Melchers, W. Camps, J. Galama, In vitro effects of sulfadiazine and its metabolites alone and in combination with pyrimethamine on Toxoplasma gondii, Antimicrobial agents and chemotherapy 39 (1995) 763-765.

[7] P.K. Borkowski, J. Brydak-Godowska, W. Basiak, M. Olszynska-Krowicka, D. Rabczenko, Adverse Reactions in Antifolate-Treated Toxoplasmic Retinochoroiditis, Current Trends in Immunity and Respiratory Infections 1108 (2018) 37-48.

[8] O.S. Adeyemi, Y. Murata, T. Sugi, K. Kato, Inorganic nanoparticles kill Toxoplasma gondii via changes in redox status and mitochondrial membrane potential, International Journal of Nanomedicine 12 (2017) 1647-1661.

[9] A.J. Hall, M.J. Chappell, J.A.D. Aston, S.A. Ward, Pharmacokinetic modelling of the anti-malarial drug artesunate and its active metabolite dihydroartemisinin, Computer Methods and Programs in Biomedicine 112 (2013) 1-15.

[10] P. Lu, S. Yao, J. Cai, P.-h. Yang, Synthesis and synergetic anti-tumor activity evaluation of dihydroartemisinin-organogermanium(IV) compound, Bioorg Med Chem Lett 24 (2014) 5294-5297.

[11] L. Cao, W.S. Duanmu, Y. Yin, Z.H. Zhou, H.F. Ge, T.A. Chen, L. Tan, A.Y. Yu, R. Hu, F. Li, H. Feng, Dihydroartemisinin exhibits anti-glioma stem cell activity through inhibiting p-AKT and activating caspase-3, Pharmazie 69 (2014) 752-758.

[12] A. Flobinus, N. Taudon, M. Desbordes, B. Labrosse, F. Simon, M.C. Mazeron, N. Schnepf, Stability and antiviral activity against human cytomegalovirus of artemisinin derivatives, Journal of Antimicrobial Chemotherapy 69 (2014) 34-40.

[13] M.E. Sarciron, C. Saccharin, A.F. Petavy, F. Peyron, Effects of artesunate, dihydroartemisinin, and an artesunate-dihydroartemisinin combination against Toxoplasma gondii, Am. J. Trop. Med. Hyg. 62 (2000) 73-76.

[14] O. Ke, E.C. Krug, J.J. Marr, R.L. Berens, Inhibition of growth of Toxoplasma gondii by qinghaosu and derivatives, Antimicrob. Agents Chemother. 34 (1990) 1961-1965.

[15] J.M. Grace, A.J. Aguilar, K.M. Trotman, T.G. Brewer, Metabolism of β-arteether to dihydroqinghaosu by human liver microsomes and recombinant cytochrome P450, Drug

Metab. Dispos. 26 (1998) 313-317.

[16] S. Vazquez-Rodriguez, R.L. Lopez, M.J. Matos, G. Armesto-Quintas, S. Serra, E. Uriarte, L. Santana, F. Borges, A.M. Crego, Y. Santos, Design, synthesis and antibacterial study of new potent and selective coumarin-chalcone derivatives for the treatment of tenacibaculosis, Bioorgan Med Chem 23 (2015) 7045-7052.

[17] Z. Chen, H. Duan, M. Wang, L. Han, Y. Liu, Y. Zhu, S. Yang, Synthesis, cytotoxicity and haemolytic activity of Pulsatilla saponin A, D derivatives, Bioorg. Med. Chem. Lett. 25 (2015) 2550-2554.

[18] Y.-N. Zhang, W. Zhang, D. Hong, L. Shi, Q. Shen, J.-Y. Li, J. Li, L.-H. Hu, Oleanolic acid and its derivatives: New inhibitor of protein tyrosine phosphatase 1B with cellular activities, Bioorg. Med. Chem. 16 (2008) 8697-8705.

[19] H.B. Zhang, Q.K. Shen, H. Wang, C. Jin, C.M. Jin, Z.S. Quan, Synthesis and evaluation of novel arctigenin derivatives as potential anti-Toxoplasma gondii agents, Eur J Med Chem 158 (2018) 414-427.

[20] S. Endo, M. Hoshi, T. Matsunaga, T. Inoue, K. Ichihara, A. Ikari, Autophagy inhibition enhances anticancer efficacy of artepillin C, a cinnamic acid derivative in Brazilian green propolis, Biochem. Biophys. Res. Commun. 497 (2018) 437-443.

[21] A. Lozynskyi, B. Zimenkovsky, R. Lesyk, Synthesis and Anticancer Activity of New Thiopyrano[2,3-d]thiazoles Based on Cinnamic Acid Amides, Sci. Pharm. 82 (2014) 723-733.

[22] A. Anwar, R. Siddiqui, M.R. Shah, N.A. Khan, Gold nanoparticle-conjugated cinnamic acid exhibits antiacanthamoebic and antibacterial properties, Antimicrob. Agents Chemother. 62 (2018) e00630-18/1-e00630-18/7.

[23] A.A. Farahat, M.A. Ismail, A. Kumar, T. Wenzler, R. Brun, A. Paul, W.D. Wilson, D.W. Boykin, Indole and Benzimidazole Bichalcophenes: Synthesis, DNA Binding and Antiparasitic Activity, Eur. J. Med. Chem. 143 (2018) 1590-1596.

[24] M. Reina, W. Ruiz-Mesia, L. Ruiz-Mesia, R. Martinez-Diaz, A. Gonzalez-Coloma, Indole alkaloids from Aspidosperma rigidum and A. schultesii and their antiparasitic effects, Z. Naturforsch., C: J. Biosci. 66 (2011) 225-234.

[25] G.R. Silveira, K.A. Campelo, G.R.S. Lima, L.P. Carvalho, S.S. Samarao, O. Vieira-da-Motta, L. Mathias, C.R.R. Matos, I.J.C. Vieira, E.J.T. de Melo, E.J. Maria, In vitro anti-Toxoplasma gondii and antimicrobial activity of amides derived from cinnamic acid, Molecules 23 (2018) 774/1-774/11.

[26] Q. Asgari, M.H. Motazedian, H. Keshavarz, M. Rezaeian, H. Sadeghpour, R. Miri, Anti-Toxoplasma Activity of 2-(Naphthalene-2-ylthiol)-1H Indole, Iran J Parasitol 10 (2015) 171-180.

[27] A.T. Smith, M.R. Livingston, A. Mai, P. Filetici, S.F. Queener, W.J. Sullivan, Jr., Quinoline derivative MC1626, a putative GCN5 histone acetyltransferase (HAT) inhibitor, exhibits HAT-independent activity against Toxoplasma gondii, Antimicrob. Agents Chemother. 51 (2007) 1109-1111.

[28] C. Jin, K. Kaewintajuk, J. Jiang, W. Jeong, M. Kamata, H.S. Kim, Y. Wataya, H. Park, Toxoplasma gondii: A simple high-throughput assay for drug screening in vitro, Experimental Parasitology 121 (2009) 132-136.

[29] M. Hollands, J.E. Logan, An Examination of Commercial Kits for the Determination of Glutamic Oxaloacetic Transaminase (GOT) and Glutamic Pyruvic Transaminase (GPT) in Serum, Can Med Assoc J 95 (1966) 303-306.

[30] E. Beutler, O. Duron, B.M. Kelly, Improved method for the determination of blood glutathione, The Journal of laboratory and clinical medicine 61 (1963) 882-888.

[31] H. Ohkawa, N. Ohishi, K. Yagi, Assay for lipid peroxides in animal tissues by thiobarbituric acid reaction, Analytical biochemistry 95 (1979) 351-358.

[32] H.B. Zhang, Q.K. Shen, H. Wang, C.M. Jin, C.M. Jin, Z.S. Quan, Synthesis and evaluation of novel arctigenin derivatives as potential anti-Toxoplasma gondii agents, European Journal of Medicinal Chemistry 158 (2018) 414-427.

[33] T. Luan, C. Jin, C.M. Jin, G.H. Gong, Z.S. Quan, Synthesis and biological evaluation of ursolic acid derivatives bearing triazole moieties as potential anti-Toxoplasma gondii agents, J Enzyme Inhib Med Chem 34 (2019) 761-772.

[34] W.H. Choi, I.A. Lee, Evaluation of Anti-Toxoplasma gondii Effect of Ursolic Acid as a Novel Toxoplasmosis Inhibitor, Pharmaceuticals (Basel) 11 (2018).

[35] C.H. Lin, Y.H. Kuo, C.C. Shih, Antidiabetic and hypolipidemic activities of eburicoic acid, a triterpenoid compound from Antrodia camphorata, by regulation of Akt phosphorylation, gluconeogenesis, and PPAR in streptozotocin-induced diabetic mice, Rsc Adv 8 (2018) 20462-20476.

[36] D.J. Creek, E. Ryan, W.N. Charman, F.C.K. Chiu, R.J. Prankerd, J.L. Vennerstrom, S.A. Charman, Stability of Peroxide Antimalarials in the Presence of Human Hemoglobin, Antimicrobial Agents and Chemotherapy 53 (2009) 3496-3500.

[37] V.R. Dola, A. Soni, P. Agarwal, H. Ahmad, K.S.R. Raju, M. Rashid, M. Wahajuddin, K. Srivastava, W. Haq, A.K. Dwivedi, S.K. Puri, S.B. Katti, Synthesis and evaluation of chirally defined side chain variants of 7-chloro-4-aminoquinoline to overcome drug resistance in malaria

chemotherapy, Antimicrob. Agents Chemother. 61 (2017) e01152-16/1-e01152-16/26.

[38] T. Choi, E. Ma, Structural necessity of indole C5-O-substitution of seco-duocarmycin analogs for their cytotoxic activity, Molecules 15 (2010) 7971-7984.

[39] X. Li, J. Sheng, G. Huang, R. Ma, F. Yin, D. Song, C. Zhao, S. Ma, Design, synthesis and antibacterial activity of cinnamaldehyde derivatives as inhibitors of the bacterial cell division protein FtsZ, Eur. J. Med. Chem. 97 (2015) 32-41.

[40] J.H. Jiang, C.M. Jin, Y.C. Kim, H.S. Kim, W.C. Park, H. Park, Anti-toxoplasmosis Effects of Oleuropein Isolated from Fraxinus rhychophylla, Biological & Pharmaceutical Bulletin 31 (2008) 2273-2276.

[41] P. Ashok, S. Chander, T.K. Smith, R.P. Singh, P.N. Jha, M. Sankaranarayanan, Biological evaluation and structure activity relationship of 9-methyl-1-phenyl-9H-pyrido[3,4-b]indole derivatives as anti-leishmanial agents, Bioorganic Chemistry 84 (2019) 98-105.

[42] A.K. Singh, V. Raj, S. Saha, Indole-fused azepines and analogues as anticancer lead molecules: Privileged findings and future directions, European Journal of Medicinal Chemistry 142 (2017) 244-265.

[43] J.P. Dubey, History of the discovery of the life cycle of Toxoplasma gondii, Int J Parasitol 39 (2009) 877-882.

[44] D.G. Mordue, F. Monroy, M. La Regina, C.A. Dinarello, L.D. Sibley, Acute toxoplasmosis leads to lethal overproduction of Th1 cytokines, J. Immunol. 167 (2001) 4574-4584.

[45] E.B. Znalesniak, T. Fu, F. Salm, U. Haendel, W. Hoffmann, Transcriptional responses in the murine spleen after toxoplasma gondii infection: inflammasome and mucus-associated genes, Int. J. Mol. Sci. 18 (2017) 1245/1-1245/11.

[46] B. Autier, S. Dion, F. Robert-Gangneux, The liver as an organ at risk for Toxoplasma transmission during transplantation: myth or reality?, J. Clin. Pathol. 71 (2018) 763-766.

[47] M.O. Dillioglugil, H.M. Kir, C. Demir, G. Ilbay, D. Sahin, O. Dillioglugil, G. Bambal, H. Mekik, N. Ates, Effect of pentylenetetrazole and sound stimulation induced single and repeated convulsive seizures on the MDA, GSH and NO levels, and SOD activities in rat liver and kidney tissues, Brain Res Bull 83 (2010) 356-359.

[48] O. Kucera, R. Endlicher, D. Rychtrmoc, H. Lotkova, O. Sobotka, Z. Cervinkova, Acetaminophen toxicity in rat and mouse hepatocytes in vitro, Drug Chem Toxicol 40 (2017) 448-456.

[49] A. Atilla, S. Aydin, A.N. Demirdoven, S.S. Kilic, Severe Toxoplasmic Hepatitis in an Immunocompetent Patient, Jpn J Infect Dis 68 (2015) 407-409.

[50] E.S. Neves, L.N. Bicudo, A.L. Curi, E. Carregal, W.F. Bueno, R.G. Ferreira, M.R. Amendoeira, E. Benchimol, O. Fernandes, Acute acquired toxoplasmosis: clinical-laboratorial aspects and ophthalmologic evaluation in a cohort of immunocompetent patients, Mem I Oswaldo Cruz 104 (2009) 393-396.

[51] W.H. Wang, F.F. Feng, J.H. Lv, Z.X. Xie, J. Chen, L.F. Zhang, W.S. Li, Major Immunodominant Region of Hepatitis B Virus Core Antigen as a Delivery Vector to Improve the Immunogenicity of the Fusion Antigen ROP2-SAG1 Multiepitope from Toxoplasma gondii in Mice, Viral Immunol 30 (2017) 508-515.

[52] J. Macias-Barragan, A. Caligiuri, J. Garcia-Banuelos, M. Parola, M. Pinzani, J. Armendariz-Borunda, [Effects of alpha lipoic acid and pirfenidone on liver cells antioxidant modulation against oxidative damage], Rev Med Chil 142 (2014) 1553-1564.

[53] K.-A. Gray, K.J. Gresty, N. Chen, V. Zhang, C.E. Gutteridge, C.L. Peatey, M. Chavchich, N.C.

Waters, Q. Cheng, Correlation between cyclin dependent kinases and artemisinin-induced dormancy in Plasmodium falciparum in vitro, PLoS One 11 (2016) e0157906/1-e0157906/14.

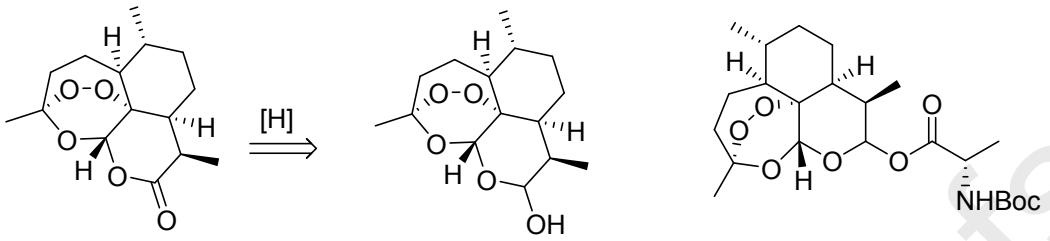

Fig. 1. a. Artemisinin and DHA b. Compound A2

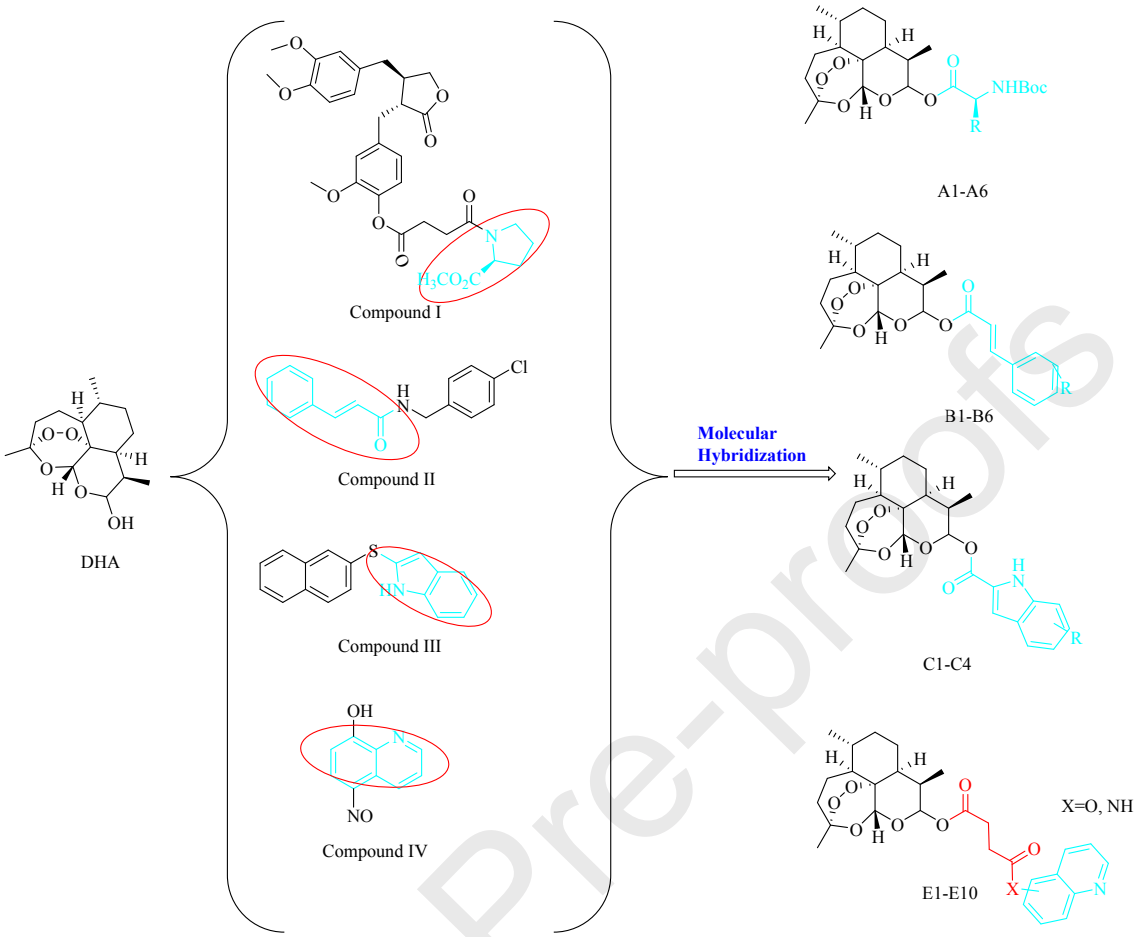

Fig. 2. Design of target compounds based on the combination principles.

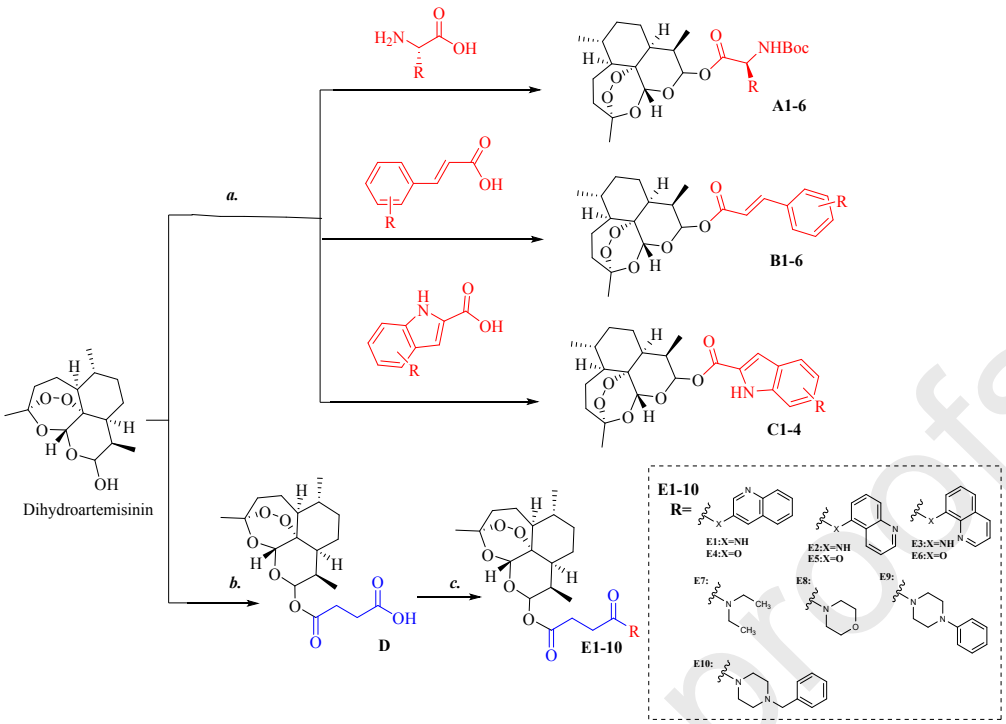

Scheme 1. Reagents and conditions for the synthesis of DHA derivatives: **a.** EDCI, DMAP, DCM, r.t.; **b.** Succinic anhydride, piperidine, ice bath; **c.** RH, EDCI, DMAP, DCM, r.t..

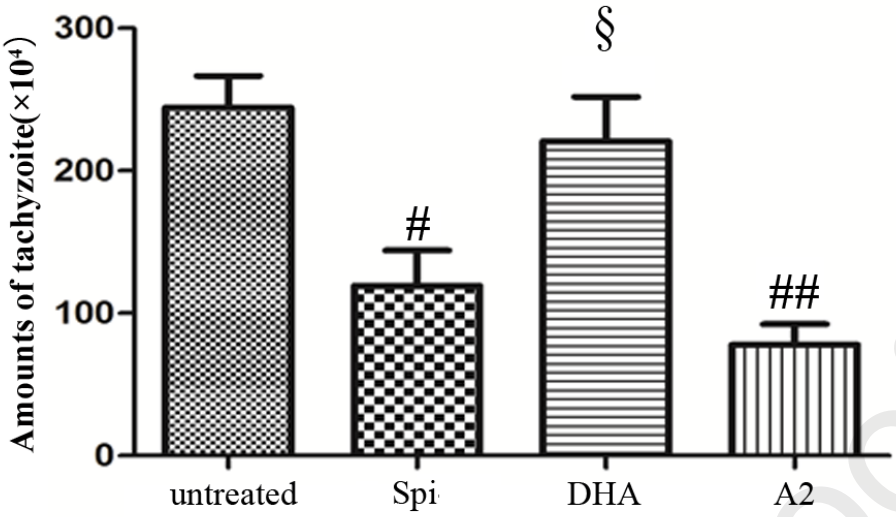

Fig. 3. Effect of compounds on the number of tachyzoites in mice, n = 6, #p<0.05 compared with untreated group; ##p<0.01 compared with untreated group; §p<0.05 compared with spi group.

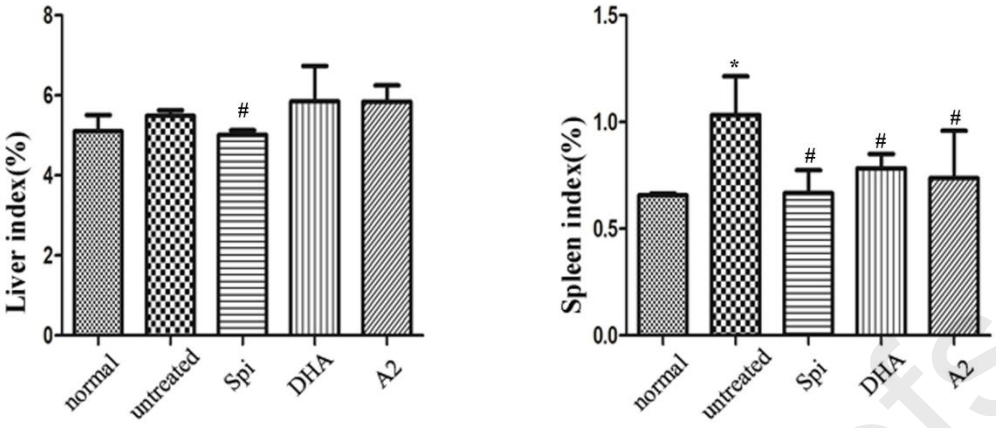

Fig. 4. Effect of compounds on spleenand liver weights in *T.gondii*-infected KM mice, n =6, #p<0.05 compared with untreated group; *p<0.05 compared with the normal group.

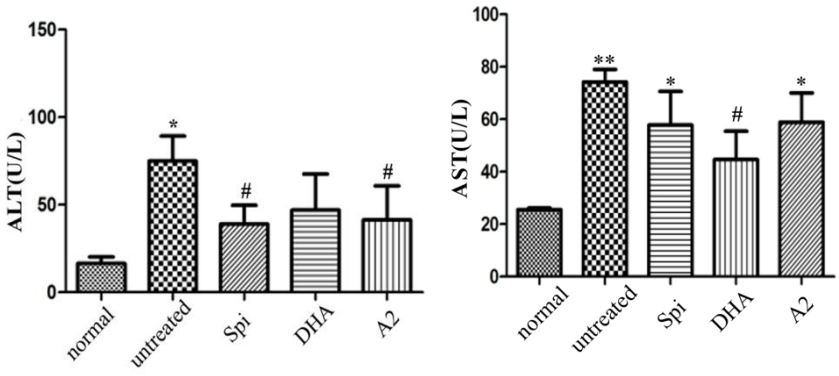

Fig. 5. Effect of compounds on ALT and AST levels in *T. gondii*-infected KM mice, n = 6,**p*<0.05compared with the normal group; ***p*<0.01 compared with the normal group; #*p*<0.05 compared with untreated group.

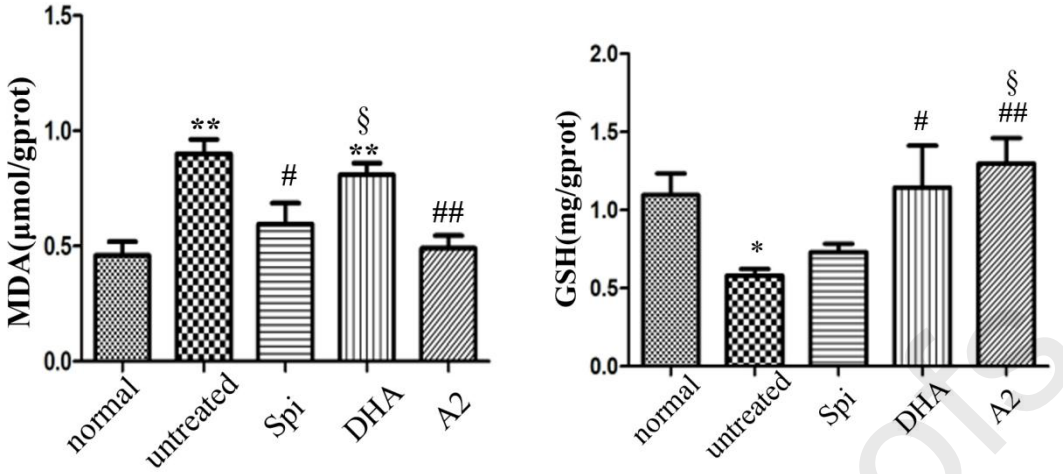

Fig. 6. Effect of compounds on GSH and MDA levels in *T.gondii*-infected KM mice, *$p < 0.05$ compared with the normal group; **$p < 0.01$ compared with the normal group; #$p < 0.05$ compared with untreated group; ##$p < 0.01$ compared with untreated group; §$p < 0.05$compared with spi group.

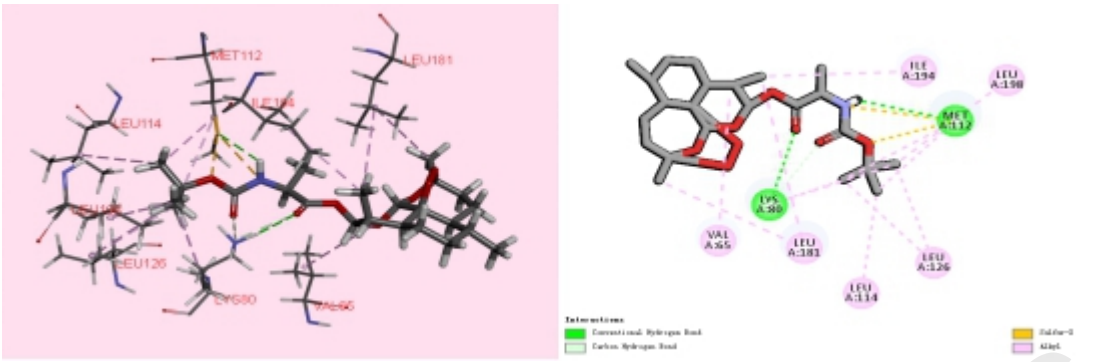

Fig. 7. Profile of compound A2 in the *Tg*CDPK1-ATP pocket (3N51.pdb).

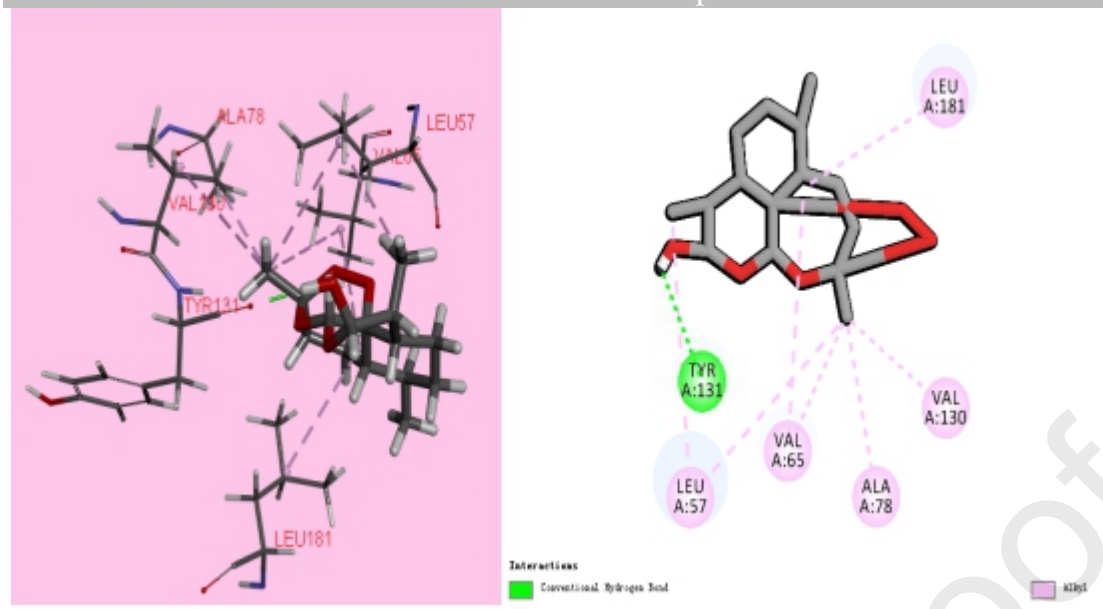

Fig. 8. Profile of DHA in the *Tg*CDPK1-ATP pocket (3N51.pdb).

Table 1. Substituents of target compounds

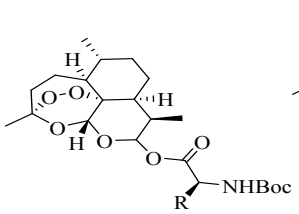

A1-6

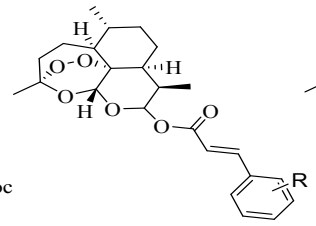

B1-6

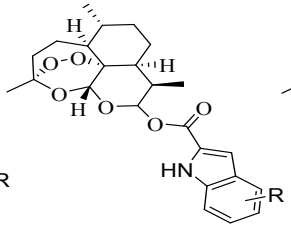

C1-4

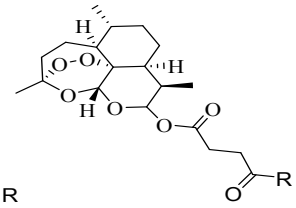

E1-10

Compd.	R	Compd.	R	Compd.	R	Compd.	R
A1		B2	*p*-F	C3	6-Br	E6	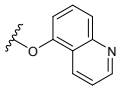
A2		B3	*p*-Cl	C4	5- OCH_3	E7	
A3	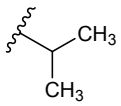	B4	*p*-Br	E1	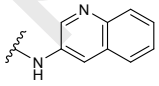	E8	
A4	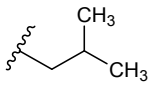	B5	*p*-OCH_3	E2	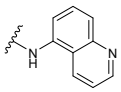	E9	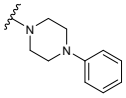
A5	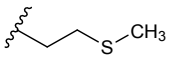	B6	3,4-diOCH_3	E3	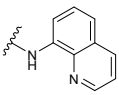	E10	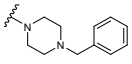
A6	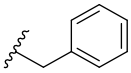	C1	5-H	E4	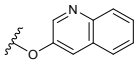		
B1	-H	C2	5-Cl	E5	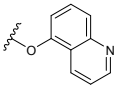		

Table 2. In vitro *T. gondii* inject-inhibition on host cells and cytotoxicity of Compounds.

Compound	IC50 in HeLa Cells (μM)[a]	IC50 in *T.gondii*-infected HeLa cells (μM)[b]	Selectivity[c]
A1	654.0 ± 18.2	448.0 ± 5.3	1.46
A2	912.1 ± 16.3	141.0 ± 2.8	6.44
A3	353.3 ± 15.1	502.7 ± 13.6	0.70
A4	>1000	946.8 ± 28.2	0.95
A5	740.0 ± 20.8	340.2 ± 24.3	2.17
A6	266.5 ± 21.0	>1000	0.27
B1	>1000	946.8 ± 18.2	1.06
B2	272.9 ± 9.8	>1000	0.27
B3	740.2 ± 17.8	340.5 ± 11.5	2.17
B4	350.2 ± 18.5	242.9 ± 8.9	1.45
B5	312.5 ± 12.6	589.0 ± 14.3	0.53
B6	674.5 ± 16.2	>1000	0.68
C1	179.0 ± 11.2	216.8 ± 13.4	0.83
C2	134.2 ± 8.3	85.3 ± 5.9	1.58
C3	170.7 ± 5.8	188.6 ± 9.9	0.91
C4	180.4 ±15.8	389.3 ± 21.0	0.46
E1	870.1 ± 22.1	217.2 ± 12.2	4.01
E2	478.3 ± 8.2	303.2 ± 10.3	1.58
E3	839.1 ± 14.8	>1000	0.84
E4	214.0 ± 11.5	210.2 ± 15.6	1.02
E5	192.6 ± 7.2	452.8 ± 13.9	0.43
E6	329.1 ± 19.9	323.4 ± 18.5	1.02
E7	557.4 ± 10.0	260.4 ± 11.2	2.14
E8	434.3 ± 18.2	473.2 ± 13.8	0.92
E9	>1000	808.9 ± 18.2	1.24
E10	797.0 ± 19.5	279.6 ± 9.4	2.85
spiramycin	189.0 ±2.1	262.2 ± 7.5	0.72
DHA	311.0 ± 11.7	311.3 ± 8.8	1.00

a = Median toxicity dose, a measure of cytotoxicity against host cells.

b = Median inhibitory concentration, a measure of tachyzoite inhibition.

c = Therapeutic index, a measure of efficacy, calculated by IC_{50} in HeLa cells/IC_{50} in *T.gondii*. When IC_{50} in HeLa cells > 1000.00, Selectivity =1000/IC_{50} in *T.gondii*; When IC_{50} in *T.gondii* > 1000.00; Selectivity = IC_{50} in HeLa cells/1000

Table 3. Mice peritoneal *T. gondii* inhibition rate

	Spi	DHA	A2
Mice peritoneal *T. gondii* inhibition rate(%)[a]	53.1% ± 11.1%	40.6% ± 13.3%	70.8% ± 4.2%

a = (untreated group - treated group) / untreated group × 100%

Table 4. The data of *molecular docking* results

Compound	-CDOCKER Interaction energy (kcal/mol)	Hydrogen bond	Carbon-hydrogen bond
		Residue/bond lengths	Residue/bond lengths
A2	50.9219	LYS80/3.07 MET112/2.87	MET112/3.05 MET112/2.39
DHA	28.4487	TRY131/1.89	

Graphical abstract

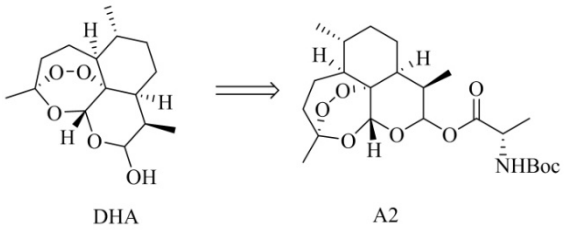

DHA A2

IC_{50} in HeLa Cells: 311 μM	IC_{50} in HeLa Cells: 912 μM
IC_{50} in T. gondii: 311 μM	IC_{50} in T. gondii: 141 μM
SI: 1.00	SI: 6.44

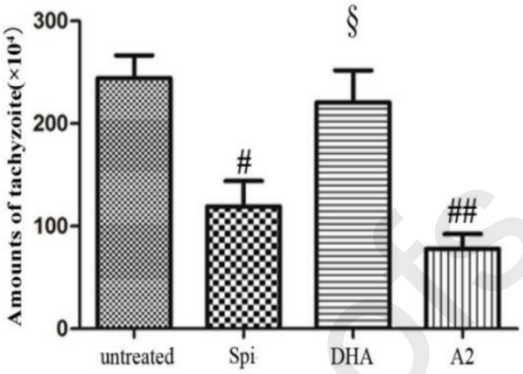

Highlights

- Four series of dihydroartemisinin derivatives were synthesized, and evaluated for their anti-*T. gondii* activity *in vitro*.
- Compound A2 were found to be the better anti-*T. gondii* activity than the lead compound and the positive drug in *in vitro* and *in vivo*.
- Compound A2 had better growth inhibitory effects on *T. gondii in vivo* than spiramycin did and significantly reduced the number of tachyzoites in the peritoneal cavity of mice ($P < 0.01$).

Conflicts of interest

The authors declare that no competing interests exist.